Citation
Su, Q. and Rong, Y. 2019. Two-Hop AF MIMO Relay System Optimization With Own Information From the Relay Node. IEEE Transactions on Signal Processing. 67 (4): pp. 930-945. http://doi.org/10.1109/TSP.2018.2885497

Two-hop AF MIMO Relay System Optimization with Own information from the Relay Node

Qiao Su and Yue Rong, *Senior Member, IEEE*

***Abstract*—In this paper, we consider precoding matrices optimization for a new two-hop amplify-and-forward (AF) multiple-input multiple-output (MIMO) relay system, where in addition to forwarding the source signals, the relay node concurrently transmits its own signals to the destination node. Compared with conventional AF MIMO relay systems where the relay node only forwards the source signals, the transceiver optimization problem in the new system is more challenging to solve. We prove that for all Schur-concave objective functions, the optimal source and relay matrices jointly diagonalize the source-relay-destination and relay-destination channels, which simplifies the matrices optimization problem to a joint subchannel and power allocation problem with scalar variables. It is shown that to achieve a maximal sum mutual information (MI) of both the source and relay links, the strongest subchannels of the second-hop channel should be allocated for transmitting signals from the relay node. With additional quality-of-service constraints in terms of the lower bounds of the MI of both links, the optimal subchannel allocation problem is NP-hard. In this case, we propose a suboptimal channel allocation algorithm with a low computational complexity. For a given subchannel allocation, we develop a primal decomposition based algorithm to efficiently solve the power allocation problem. Simulation results show that compared with the exhaustive search based channel allocation approach and the general nonlinear programming based power allocation algorithm, the proposed subchannel and power allocation algorithms have a much lower computational complexity with only a small performance loss.**

***Index Terms*—Amplify-and-forward, MIMO relay, power allocation, precoding matrix, quality-of-service, subchannel allocation.**

I. Introduction

Wireless relay communication has attracted much interest recently from both academia and industry due to its potential in increasing the coverage and capacity of wireless communication systems, particularly in shadowed environments [1]-[3]. Several relay protocols such as amplify-and-forward (AF) and decode-and-forward (DF) have been developed [1]. Compared with the DF protocol where the relay nodes first decode and then re-encode the received signals, in an AF relay system, the relay node simply performs a linear transformation of the received signals. Therefore, the complexity of the AF protocol is much lower than that of the DF protocol, particularly when multiple-input multiple-output (MIMO) relay systems are considered [4].

This work is supported by the Australian Research Council's Discovery Projects funding scheme (DP140102131).

Q. Su is with the College of Communications Engineering, Army Engineering University of PLA, Nanjing, China (e-mail: qiaosu810@foxmail.com).

Y. Rong is with the School of Electrical Engineering, Computing and Mathematical Sciences, Curtin University, Bentley, WA, Australia (e-mail: y.rong@curtin.edu.au).

Capacity bounds of AF MIMO relay systems have been studied in [5]. The relay precoding matrix which maximizes the source-destination mutual information (MI) of a two-hop AF MIMO relay system has been investigated in [6] and [7]. In [8] and [9], the relay precoding matrix that minimizes the mean-squared error (MSE) of the signal waveform estimation has been proposed. In [10], a unified framework has been established to jointly optimize the source and relay precoding matrices of AF MIMO relay systems with a broad class of commonly used objective functions. Joint source and relay matrices optimization with the direct source-destination link has been investigated in [11] and [12]. In [13] and [14], precoding techniques for AF MIMO relay systems with a decision feedback receiver have been studied. Taking into account the mismatch between the true and the estimated channel state information (CSI), robust transceiver design algorithms for AF MIMO relay systems have been proposed in [15]-[17]. The quality-of-service (QoS)-constrained source and relay precoding matrices design has been studied in [18]-[20].

It is worth noting that for the MIMO relay systems considered in [6]-[20], the relay node only forwards signals from the source node to the destination node and does not transmit its own signals. However, in many scenarios the relay node needs to transmit its own signals to the destination node. For example, in the uplink of a cellular system where the base station (BS) is the destination node, a mobile terminal close to the BS can serve as a relay node to assist the communication between a user located at the edge of the cell and the BS. Meanwhile, this mobile terminal needs to send it own message to the BS.

Considering this important practical requirement above, in this paper, we investigate precoding matrices optimization for a new two-hop AF MIMO relay system, where in addition to forwarding the source signals, the relay node concurrently transmits its own signals to the destination node. To the best of our knowledge, there is no other work in open literature which studied the transceiver optimization problem for such AF MIMO relay system. Compared with conventional AF MIMO relay systems where the relay node only forwards the source signals [6]-[20], the transceiver optimization problem in the new system is more challenging to solve. Compared with multiuser AF relay systems [21]-[23], where the signals from different users are precoded by a same relay matrix, in this new relay system, the source signals and relay signals are precoded by different matrices at the relay node. Therefore, the relay system studied in this paper is more general than a multiuser AF relay system.

We prove that for all Schur-concave [24] objective functions, the optimal source and relay matrices jointly diagonalize the source-relay-destination channel (for signals from the source node) and the relay-destination channel (for signals of the relay node). This new result generalizes the outcomes in [6]-[10] and [21]-[23] from conventional AF MIMO relay channels to systems where the relay node also transmits its own signals.

By exploiting the optimal structure of the source and relay precoding matrices, the original matrices optimization problem is simplified to a joint subchannel and power allocation problem with scalar variables. We prove that to achieve a maximal sum MI of both the source and relay links, the strongest subchannels of the second-hop channel should be allocated for transmitting signals from the relay node. With a given subchannel allocation, the original transceiver optimization problem boils down to a power allocation problem. We develop a primal decomposition [25] based algorithm to efficiently solve the power allocation problem.

Note that the maximal sum MI criterion might lead to fairness issues, as the source signals are assigned with weaker second-hop subchannels compared with those allocated to the relay signals. To solve this problem, we impose additional QoS constraints in terms of the lower bounds of the MI of both links. However, with these QoS constraints, the optimal subchannel allocation problem becomes NP-hard. In this case, we propose a suboptimal channel allocation algorithm with a low computational complexity. For a given channel allocation scheme, we derive the achievable rate region for the source and relay signals. Based on the rate region, an efficient power allocation algorithm is developed using the primal decomposition technique. Simulation results show that compared with the exhaustive search based channel allocation approach and the general nonlinear programming based power allocation algorithm, the proposed subchannel and power allocation algorithms have a much lower computational complexity with only a small performance loss.

The rest of this paper is organized as follows. In Section II, the system model of a two-hop AF MIMO relay system with own information from the relay node is presented. The proposed transceiver design algorithm is developed in Section III. In Section IV, QoS constraints are considered. Simulation results are shown in Section V to validate the performance of the proposed algorithms. Finally, conclusions are drawn in Section VI.

II. System Model

We consider a two-hop AF relay system, where the source node sends information to the destination node with the aid of a MIMO relay node. Different to conventional AF MIMO relay systems, in addition to forwarding the source information to the destination node, the relay node also needs to transmit its own information to the destination node as shown in Fig. 1. We assume that the source, relay, and destination nodes are equipped with N_s, N_r, and N_d antennas, respectively. Similar to [6], [8], [10], the direct link between the source and destination nodes is not considered, as we assume that

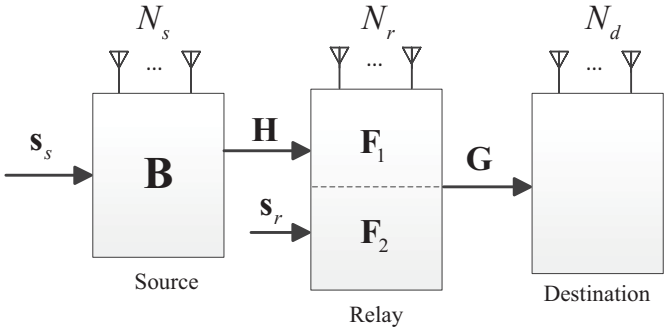

Fig. 1. System block diagram of an AF MIMO relay system where the relay node transmits own information to the destination node.

the effects of path attenuation and shadowing are more severe on the direct link compared with the link via the relay node.

Using a practical half-duplex relay node, the communication process is completed in two time slots. At the first time slot, the source node linearly precodes the $N_1 \times 1$ information-carrying vector $\mathbf{s}_s$ with an $N_s \times N_1$ matrix $\mathbf{B}$ and transmits

$$\mathbf{x}_s = \mathbf{B}\mathbf{s}_s \tag{1}$$

to the relay node. We assume that $E\{\mathbf{s}_s\mathbf{s}_s^H\} = \mathbf{I}_{N_1}$, where $E\{\cdot\}$ stands for the statistical expectation, $(\cdot)^H$ stands for the matrix Hermitian transpose, and $\mathbf{I}_n$ denotes the $n \times n$ identity matrix. The received signal vector at the relay node is given by

$$\begin{aligned}\mathbf{y}_r &= \mathbf{H}\mathbf{x}_s + \mathbf{n}_r \\ &= \mathbf{H}\mathbf{B}\mathbf{s}_s + \mathbf{n}_r\end{aligned} \tag{2}$$

where $\mathbf{H}$ is the $N_r \times N_s$ source-relay MIMO channel matrix and $\mathbf{n}_r$ is the $N_r \times 1$ noise vector at the relay node.

At the second time slot, the relay node linearly precodes $\mathbf{y}_r$ with an $N_r \times N_r$ matrix $\mathbf{F}_1$ and superimposes its own $N_2 \times 1$ information-carrying vector $\mathbf{s}_r$ precoded by an $N_r \times N_2$ matrix $\mathbf{F}_2$. We assume that $E\{\mathbf{s}_r\mathbf{s}_r^H\} = \mathbf{I}_{N_2}$ and $\mathbf{s}_r$ is independent of $\mathbf{s}_s$. Using (2), the signal vector transmitted by the relay node is given by

$$\begin{aligned}\mathbf{x}_r &= \mathbf{F}_1\mathbf{y}_r + \mathbf{F}_2\mathbf{s}_r \\ &= \mathbf{F}_1\mathbf{H}\mathbf{B}\mathbf{s}_s + \mathbf{F}_2\mathbf{s}_r + \mathbf{F}_1\mathbf{n}_r.\end{aligned} \tag{3}$$

The signal vector received at the destination node is

$$\begin{aligned}\mathbf{y}_d &= \mathbf{G}\mathbf{x}_r + \mathbf{n}_d \\ &= [\mathbf{G}\mathbf{F}_1\mathbf{H}\mathbf{B}, \quad \mathbf{G}\mathbf{F}_2]\begin{bmatrix}\mathbf{s}_s \\ \mathbf{s}_r\end{bmatrix} + \mathbf{G}\mathbf{F}_1\mathbf{n}_r + \mathbf{n}_d \\ &= \mathbf{M}\mathbf{s} + \mathbf{n}\end{aligned} \tag{4}$$

where $\mathbf{G}$ is the $N_d \times N_r$ relay-destination channel matrix, $\mathbf{n}_d$ is the $N_d \times 1$ noise vector at the destination node, and

$$\mathbf{M} = [\mathbf{G}\mathbf{F}_1\mathbf{H}\mathbf{B},\ \mathbf{G}\mathbf{F}_2],\ \mathbf{s} = [\mathbf{s}_s^T, \mathbf{s}_r^T]^T,\ \mathbf{n} = \mathbf{G}\mathbf{F}_1\mathbf{n}_r + \mathbf{n}_d$$

are the equivalent MIMO channel matrix, the total information signal vector, and the equivalent noise vector, respectively. Here $(\cdot)^T$ denotes the matrix (vector) transpose.

We assume that $\mathbf{n}_r$ and $\mathbf{n}_d$ are independent and identically distributed (i.i.d.) Gaussian noise vectors with zero-mean and

unit variance entries. We also assume a perfect knowledge on the CSI of $\mathbf{H}$ and $\mathbf{G}$. In practice, $\mathbf{H}$ and $\mathbf{G}$ can be estimated, for example, using the approaches in [26] and [27]. It is worth noting that (4) presents a general model for a two-hop AF MIMO relay system without the direct link. Conventional AF MIMO systems [6]-[10] where the relay node does not transmit its own information corresponds to (4) with $\mathbf{F}_2 = \mathbf{0}$. We can also view (4) as a two-user AF MIMO relay system [21]-[23], where $\mathbf{s}_r$ can be viewed as signals from one user with an ideal source-relay channel. However, different to [23], where $\mathbf{s}_s$ and $\mathbf{s}_r$ are precoded by a same matrix at the relay node, here they are precoded by different $\mathbf{F}_1$ and $\mathbf{F}_2$.

Due to its simplicity, a linear receiver is used at the destination node to retrieve the source and relay signals. Thus, the estimated signal vector can be written as

$$\hat{\mathbf{s}} = \mathbf{W}^H \mathbf{y}_d \tag{5}$$

where $\mathbf{W}$ is the $N_d \times N$ weight matrix of the receiver with $N = N_1 + N_2$. From (4) and (5), the MSE matrix of the signal waveform estimation is given by

$$\begin{aligned}\mathbf{E} &= E\{(\hat{\mathbf{s}} - \mathbf{s})(\hat{\mathbf{s}} - \mathbf{s})^H\} \\ &= (\mathbf{W}^H\mathbf{M} - \mathbf{I}_N)(\mathbf{W}^H\mathbf{M} - \mathbf{I}_N)^H + \mathbf{W}^H\mathbf{C}\mathbf{W} \end{aligned} \tag{6}$$

where $\mathbf{C} = E\{\mathbf{n}\mathbf{n}^H\} = \mathbf{G}\mathbf{F}_1\mathbf{F}_1^H\mathbf{G}^H + \mathbf{I}_{N_d}$ is the covariance matrix of $\mathbf{n}$.

It can be seen that the optimal $\mathbf{W}$ is given by

$$\mathbf{W} = (\mathbf{M}\mathbf{M}^H + \mathbf{C})^{-1}\mathbf{M} \tag{7}$$

where $(\cdot)^{-1}$ stands for the matrix inversion. By substituting (7) back into (6), we obtain

$$\begin{aligned}\mathbf{E} &= (\mathbf{I}_N + \mathbf{M}^H\mathbf{C}^{-1}\mathbf{M})^{-1} \\ &= \left(\mathbf{I}_N + \begin{bmatrix}\mathbf{B}^H\mathbf{H}^H\mathbf{F}_1^H\mathbf{G}^H \\ \mathbf{F}_2^H\mathbf{G}^H\end{bmatrix}(\mathbf{G}\mathbf{F}_1\mathbf{F}_1^H\mathbf{G}^H + \mathbf{I}_{N_d})^{-1}\right. \\ &\quad \left.\times \begin{bmatrix}\mathbf{G}\mathbf{F}_1\mathbf{H}\mathbf{B}, & \mathbf{G}\mathbf{F}_2\end{bmatrix}\right)^{-1}. \end{aligned} \tag{8}$$

Based on (1) and (3), the transmission power consumed by the source and relay nodes can be calculated respectively as

$$E\{\mathbf{x}_s\mathbf{x}_s^H\} = \mathrm{tr}(\mathbf{B}\mathbf{B}^H) \tag{9}$$

$$E\{\mathbf{x}_r\mathbf{x}_r^H\} = \mathrm{tr}(\mathbf{F}_1(\mathbf{H}\mathbf{B}\mathbf{B}^H\mathbf{H}^H + \mathbf{I}_{N_r})\mathbf{F}_1^H + \mathbf{F}_2\mathbf{F}_2^H) \tag{10}$$

where $\mathrm{tr}(\cdot)$ denotes the matrix trace.

III. Proposed Precoding Matrices Design

From (8)-(10), the source and relay precoding matrices optimization problem can be written as

$$\min_{\mathbf{F}_1,\mathbf{F}_2,\mathbf{B}} \; f(\mathbf{d}(\mathbf{E})) \tag{11}$$

$$\text{s.t. } \mathrm{tr}(\mathbf{B}\mathbf{B}^H) \le P_s \tag{12}$$

$$\mathrm{tr}(\mathbf{F}_1(\mathbf{H}\mathbf{B}\mathbf{B}^H\mathbf{H}^H + \mathbf{I}_{N_r})\mathbf{F}_1^H + \mathbf{F}_2\mathbf{F}_2^H) \le P_r \tag{13}$$

where $f(\cdot)$ stands for a unified objective function which is increasing with respect to each element of $\mathbf{d}(\mathbf{E})$, for a matrix $\mathbf{A}$, $\mathbf{d}(\mathbf{A})$ is a column vector containing all main diagonal elements of $\mathbf{A}$, P_s and P_r are the transmission powers available at the source node and the relay node, respectively. We assume that $f(\cdot)$ is Schur-concave [24] with respect to $\mathbf{d}(\mathbf{E})$. As shown in [10], a large number of commonly used objective functions in MIMO relay system design such as the arithmetic MSE and the negative MI are Schur-concave functions of $\mathbf{d}(\mathbf{E})$.

Compared with the source and relay matrices optimization problem for conventional two-hop MIMO relay systems [6]-[20], the problem (11)-(13) is more challenging to solve, because the introduction of $\mathbf{F}_2$ makes the objective function (11) and the constraint (13) more complicated. Obviously, the source and relay matrices optimization problem for conventional two-hop MIMO relay systems [6]-[10] is a special case of the problem (11)-(13) when $\mathbf{F}_2 = \mathbf{0}$.

A. Optimal Structure of Source and Relay Precoding Matrices

Let us introduce the singular value decomposition (SVD) of $\mathbf{H} = \mathbf{U}_h\mathbf{\Lambda}_h\mathbf{V}_h^H$ and $\mathbf{G} = \mathbf{U}_g\mathbf{\Lambda}_g\mathbf{V}_g^H$, where the diagonal elements of $\mathbf{\Lambda}_h$ and $\mathbf{\Lambda}_g$ are sorted in a decreasing order. The dimensions of $\mathbf{\Lambda}_h$ and $\mathbf{\Lambda}_g$ are $r_h \times r_h$ and $r_g \times r_g$, respectively, where $r_h = \mathrm{rank}(\mathbf{H})$, $r_g = \mathrm{rank}(\mathbf{G})$, and $\mathrm{rank}(\cdot)$ denotes the matrix rank. The following theorem states the optimal structure of $\mathbf{F}_1$, $\mathbf{F}_2$, and $\mathbf{B}$.

Theorem 1: We assume that $\mathrm{rank}(\mathbf{B}) = \mathrm{rank}(\mathbf{F}_1) = N_1$ and $\mathrm{rank}(\mathbf{F}_2) = N_2$ with $N_1 \le \min(r_h, r_g)$ and $N_1 + N_2 \le r_g$. The optimal source and relay matrices as the solution to the problem (11)-(13) have the following structure

$$\mathbf{F}_1 = \mathbf{V}_{g,1}\mathbf{\Lambda}_{f_1}\mathbf{U}_{h,m}^H, \; \mathbf{F}_2 = \mathbf{V}_{g,2}\mathbf{\Lambda}_{f_2}, \; \mathbf{B} = \mathbf{V}_{h,m}\mathbf{\Lambda}_b \tag{14}$$

where $\mathbf{\Lambda}_{f_1}$, $\mathbf{\Lambda}_{f_2}$, and $\mathbf{\Lambda}_b$ are $N_1 \times N_1$, $N_2 \times N_2$, and $N_1 \times N_1$ diagonal matrices, respectively, with positive diagonal elements sorted in a decreasing order, $\mathbf{V}_{g,1}$ and $\mathbf{V}_{g,2}$ contain N_1 and N_2 columns of $\mathbf{V}_g$, respectively, and together they contain N columns of $\mathbf{V}_g$ associated with the largest N singular values of $\mathbf{G}$, $\mathbf{U}_{h,m}$ and $\mathbf{V}_{h,m}$ contain N_1 columns of $\mathbf{U}_h$ and $\mathbf{V}_h$, respectively, associated with the largest N_1 singular values of $\mathbf{H}$.

Proof: See Appendix A. ∎

It can be seen from (14) that the optimal $\mathbf{F}_1$, $\mathbf{F}_2$, and $\mathbf{B}$ jointly diagonalize the source-relay-destination channel such that

$$\mathbf{M} = \mathbf{U}_{g,m}\mathbf{\Pi}\begin{bmatrix}\mathbf{\Lambda}_{g,1}\mathbf{\Lambda}_{f_1}\mathbf{\Lambda}_{h,m}\mathbf{\Lambda}_b & \mathbf{0} \\ \mathbf{0} & \mathbf{\Lambda}_{g,2}\mathbf{\Lambda}_{f_2}\end{bmatrix} \tag{15}$$

where $\mathbf{U}_{g,m}$ contains N columns of $\mathbf{U}_g$ associated with the largest N singular values of $\mathbf{G}$, $\mathbf{\Lambda}_{g,1}$ and $\mathbf{\Lambda}_{g,2}$ contain singular values from $\mathbf{\Lambda}_g$ associated with $\mathbf{V}_{g,1}$ and $\mathbf{V}_{g,2}$, respectively, and $\mathbf{\Lambda}_{h,m}$ contains the largest N_1 singular values of $\mathbf{H}$. Note that different to conventional two-hop MIMO relay systems [6]-[10], there is a permutation matrix $\mathbf{\Pi}$ in (15), as explained in Appendix A. In fact, $\mathbf{\Pi}$ reflects that in order to optimize (11), among the N strongest subchannels of $\mathbf{G}$, which N_1 subchannels should be allocated to the source signals $\mathbf{s}_s$ (with the remaining N_2 subchannels assigned to the relay signals $\mathbf{s}_r$). From Theorem 1, we have $N_1 \le \min(N_s, N_r, N_d)$ and $N_1 + N_2 \le \min(N_r, N_d)$. Thus, there are $N_s \ge N_1$, $N_r \ge N_1 + N_2$, and $N_d \ge N_1 + N_2$.

In general, the optimal structure of the source and relay precoding matrices in [10] for Schur-convex objective functions does not hold for the relay system studied in this paper. It has been shown in [10] that for a conventional two-hop AF

MIMO relay system (where the relay node does not transmit its own signals), to optimize a Schur-convex function, the source precoding matrix needs to be rotated by a unitary matrix such that the MSE matrix has identical main diagonal elements. For the relay system in this paper, as the "equivalent" source precoding matrix $\mathbf{B}_s = \begin{pmatrix} \mathbf{B} & \mathbf{0} \\ \mathbf{0} & \mathbf{F}_2 \end{pmatrix}$ has a block diagonal constraint, in general it is not possible to rotate $\mathbf{B}_s$ by a block diagonal unitary matrix such that the MSE matrix $\mathbf{E}$ has identical main diagonal elements.

Using Theorem 1, the MSE matrix (8) can be written as

$$\mathbf{E}_0 = \left(\mathbf{I}_N + \begin{bmatrix} \mathbf{\Lambda}_{g,1}^2\mathbf{\Lambda}_{f_1}^2\mathbf{\Lambda}_{h,m}^2\mathbf{\Lambda}_b^2(\mathbf{\Lambda}_{g,1}^2\mathbf{\Lambda}_{f_1}^2+\mathbf{I}_{N_1})^{-1} & \mathbf{0} \\ \mathbf{0} & \mathbf{\Lambda}_{g,2}^2\mathbf{\Lambda}_{f_2}^2 \end{bmatrix}\right)^{-1}. \tag{16}$$

The constraints (12) and (13) can be rewritten as

$$\mathrm{tr}(\mathbf{\Lambda}_b^2) \le P_s \tag{17}$$

$$\mathrm{tr}(\mathbf{\Lambda}_{f_1}^2(\mathbf{\Lambda}_{h,m}^2\mathbf{\Lambda}_b^2 + \mathbf{I}_{N_1})) + \mathrm{tr}(\mathbf{\Lambda}_{f_2}^2) \le P_r. \tag{18}$$

Using (16)-(18), the problem (11)-(13) can be written as

$$\min_{\mathcal{I},\mathcal{J},\boldsymbol{\lambda}_{f_1},\boldsymbol{\lambda}_{f_2},\boldsymbol{\lambda}_b} f\left(\left\{\left(1+\frac{\lambda_{g,\mathcal{I}_i}^2\lambda_{f_1,i}^2\lambda_{h,i}^2\lambda_{b,i}^2}{1+\lambda_{g,\mathcal{I}_i}^2\lambda_{f_1,i}^2}\right)^{-1}\right\}_{N_1}, \left\{(1+\lambda_{g,\mathcal{J}_j}^2\lambda_{f_2,j}^2)^{-1}\right\}_{N_2}\right) \tag{19}$$

$$\text{s.t.} \sum_{i=1}^{N_1}\lambda_{b,i}^2 \le P_s \tag{20}$$

$$\sum_{i=1}^{N_1}\lambda_{f_1,i}^2(\lambda_{h,i}^2\lambda_{b,i}^2+1) + \sum_{j=1}^{N_2}\lambda_{f_2,j}^2 \le P_r \tag{21}$$

$$\lambda_{f_1,i} > 0, \quad \lambda_{b,i} > 0, \quad i = 1,\cdots,N_1 \tag{22}$$

$$\lambda_{f_2,j} > 0, \quad j = 1,\cdots,N_2 \tag{23}$$

$$\underline{\mathcal{I}} = N_1, \underline{\mathcal{J}} = N_2, \mathcal{I}\cap\mathcal{J} = \emptyset, \mathcal{I}\cup\mathcal{J} = \{1,\cdots,N\} \tag{24}$$

where for variables x_i, $\{x_i\}_M \triangleq x_1,\cdots,x_M$, $\underline{\mathcal{I}}$ denotes the cardinality of set $\mathcal{I}$, set $\mathcal{I}$ and set $\mathcal{J}$ contain the indices of N_1 and N_2 subchannels in $\mathbf{G}$ that are allocated to $\mathbf{s}_s$ and $\mathbf{s}_r$, respectively, $\boldsymbol{\lambda}_{f_1} = [\lambda_{f_1,1},\cdots,\lambda_{f_1,N_1}]^T$, $\boldsymbol{\lambda}_{f_2} = [\lambda_{f_2,1},\cdots,\lambda_{f_2,N_2}]^T$, and $\boldsymbol{\lambda}_b = [\lambda_{b,1},\cdots,\lambda_{b,N_1}]^T$.

It can be seen that by using the optimal structure of $\mathbf{F}_1$, $\mathbf{F}_2$, and $\mathbf{B}$, the matrices optimization problem (11)-(13) is converted to the problem (19)-(24) with scalar variables. However, the problem (19)-(24) is a joint subchannel and power allocation problem, which is much harder to solve than the pure power allocation problem in conventional MIMO relay systems [6]-[10], as the optimal allocation of subchannels to $\mathcal{I}$ and $\mathcal{J}$ is a combinatorial problem.

By introducing $\lambda_{b,i}^2 = x_i$, $\lambda_{f_1,i}^2(\lambda_{h,i}^2\lambda_{b,i}^2+1) = y_i$, $\lambda_{h,i}^2 = a_i$, $i = 1,\cdots,N_1$, $\lambda_{f_2,j}^2 = z_j$, $j = 1,\cdots,N_2$, $\lambda_{g,k}^2 = b_k$, $k = 1,\cdots,N$, the problem (19)-(24) can be rewritten as the following joint subchannel and power allocation problem

$$\min_{\mathcal{I},\mathcal{J},\mathbf{x},\mathbf{y},\mathbf{z}} f\left(\left\{\left(1+\frac{a_ix_ib_{\mathcal{I}_i}y_i}{1+a_ix_i+b_{\mathcal{I}_i}y_i}\right)^{-1}\right\}_{N_1}, \left\{(1+b_{\mathcal{J}_j}z_j)^{-1}\right\}_{N_2}\right) \tag{25}$$

$$\text{s.t.} \sum_{i=1}^{N_1} x_i \le P_s \tag{26}$$

$$\sum_{i=1}^{N_1} y_i + \sum_{j=1}^{N_2} z_j \le P_r \tag{27}$$

$$x_i > 0, \quad y_i > 0, \quad i = 1,\cdots,N_1 \tag{28}$$

$$z_j > 0, \quad j = 1,\cdots,N_2 \tag{29}$$

$$\underline{\mathcal{I}} = N_1, \underline{\mathcal{J}} = N_2, \mathcal{I}\cap\mathcal{J} = \emptyset, \mathcal{I}\cup\mathcal{J} = \{1,\cdots,N\} \tag{30}$$

where $\mathbf{x} = [x_1,\cdots,x_{N_1}]^T$, $\mathbf{y} = [y_1,\cdots,y_{N_1}]^T$, and $\mathbf{z} = [z_1,\cdots,z_{N_2}]^T$. Note that a_i, $i = 1,\cdots,N_1$, and b_k, $k = 1,\cdots,N$, are sorted in decreasing orders, respectively.

The exact solution to the problem (25)-(30) depends on the objective function f. In the following, we adopt the commonly used maximal MI criterion with $f = \log_2|\mathbf{E}_0|$, which is a Schur-concave function of $\mathbf{d}(\mathbf{E}_0)$ [10]. Here $|\cdot|$ denotes the matrix determinant. Then the problem (25)-(30) can be written as

$$\max_{\mathcal{I},\mathcal{J},\mathbf{x},\mathbf{y},\mathbf{z}} \sum_{i=1}^{N_1}\log_2\left(1+\frac{a_ix_ib_{\mathcal{I}_i}y_i}{1+a_ix_i+b_{\mathcal{I}_i}y_i}\right) + \sum_{j=1}^{N_2}\log_2(1+b_{\mathcal{J}_j}z_j) \tag{31}$$

$$\text{s.t.} \sum_{i=1}^{N_1} x_i \le P_s \tag{32}$$

$$\sum_{i=1}^{N_1} y_i + \sum_{j=1}^{N_2} z_j \le P_r \tag{33}$$

$$x_i > 0, \quad y_i > 0, \quad i = 1,\cdots,N_1 \tag{34}$$

$$z_j > 0, \quad j = 1,\cdots,N_2 \tag{35}$$

$$\underline{\mathcal{I}} = N_1, \underline{\mathcal{J}} = N_2, \mathcal{I}\cap\mathcal{J} = \emptyset, \mathcal{I}\cup\mathcal{J} = \{1,\cdots,N\}. \tag{36}$$

Interestingly, we can see that the first summation in (31) is the MI between $\mathbf{s}_s$ and $\mathbf{y}_d$, while the second summation is the MI between $\mathbf{s}_r$ and $\mathbf{y}_d$. Thus, (31) is the sum MI of both the source and relay links.

B. Optimal Subchannel Allocation

Theorem 2: The optimal subchannel allocation for the problem (31)-(36) is $\mathcal{I} = \{N_2+1,\cdots,N\}$ and $\mathcal{J} = \{1,\cdots,N_2\}$ for any $\mathbf{H}$ and $\mathbf{G}$.

Proof: See Appendix B. ■

Theorem 2 indicates that to maximize the sum MI (31), the N_2 strongest subchannels of $\mathbf{G}$ (i.e., $b_1,\cdots,b_{N_2}$) should be allocated to $\mathbf{s}_r$ and the N_1 second strongest subchannels of $\mathbf{G}$ (i.e., $b_{N_2+1},\cdots,b_N$) are assigned to $\mathbf{s}_s$. This subchannel allocation is optimal for any realization of $\mathbf{H}$ and $\mathbf{G}$.

Let us denote $\{\mathcal{A}|\mathcal{B}\}$ as a subchannel allocation where $\mathcal{A} = \{b_{\mathcal{J}_j}, j = 1,\cdots,N_2\}$ and $\mathcal{B} = \{b_{\mathcal{I}_i}, i = 1,\cdots,N_1\}$ are assigned to $\mathbf{s}_r$ and $\mathbf{s}_s$, respectively. Now we analyze the impact of subchannel allocation on the sum MI using a simple example of $N_1 = 3$ and $N_2 = 2$. In this example, there are altogether 10 possible subchannel allocations as

$$\begin{aligned} &①=\{b_1,b_2|b_3,b_4,b_5\}, \quad ②=\{b_1,b_3|b_2,b_4,b_5\} \\ &③=\{b_1,b_4|b_2,b_3,b_5\}, \quad ④=\{b_1,b_5|b_2,b_3,b_4\} \\ &⑤=\{b_2,b_3|b_1,b_4,b_5\}, \quad ⑥=\{b_2,b_4|b_1,b_3,b_5\} \\ &⑦=\{b_2,b_5|b_1,b_3,b_4\}, \quad ⑧=\{b_3,b_4|b_1,b_2,b_5\} \\ &⑨=\{b_3,b_5|b_1,b_2,b_4\}, \quad ⑩=\{b_4,b_5|b_1,b_2,b_3\}. \end{aligned} \tag{37}$$

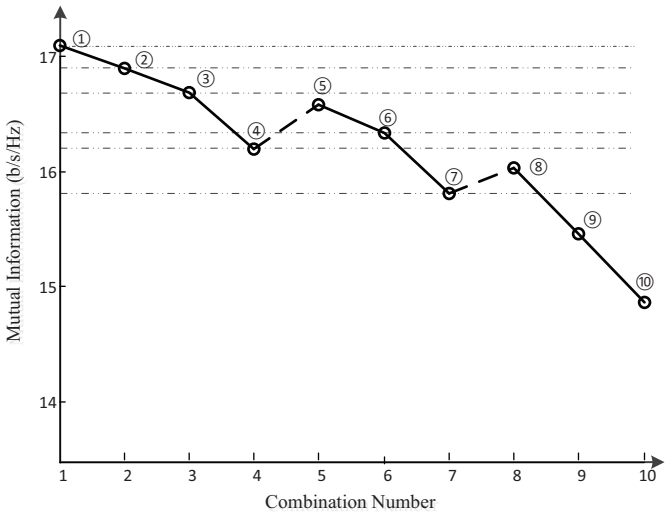

Fig. 2. Sum MI at all subchannel allocation schemes. $N_s = 3$, $N_r = 5$, $N_d = 5$, $N_1 = 3$, $N_2 = 2$, and $\mathrm{SNR}_s = \mathrm{SNR}_r = 20$ dB.

The maximal values of the objective function (31) with these 10 subchannel allocations are shown in Fig. 2 for a MIMO relay system with $N_s = 3$, $N_r = 5$, $N_d = 5$ and a typical channel realization of $\mathbf{H}$ and $\mathbf{G}$, where the numbers ① to ⑩ correspond to the 10 allocations listed above. Here the signal-to-noise ratio (SNR) of the first-hop channel SNR_s and the second-hop channel SNR_r are both set to 20 dB. It can be clearly seen from Fig. 2 that the subchannel allocation ① leads to the largest sum MI, which corroborates Theorem 2.

The solid lines in Fig. 2 show that the sum MI decreases along ①-④, ⑤-⑦, and ⑧-⑩. This can be proven by the results in Appendix B that if we swap $b_{\mathcal{I}_i}$ with $b_{\mathcal{J}_j}$ where $b_{\mathcal{I}_i} < b_{\mathcal{J}_j}$, then the maximal value of the objective function (31) will decrease. For instance, ③ is obtained by swapping b_3 and b_4 in ②. Thus, the sum MI achieved by ③ is smaller than ②. Using this reasoning, we can prove that the sum MI achieved by ⑤ is smaller than ②, as the former allocation is obtained by swapping b_1 with b_2 from the latter one. However, based on Appendix B we cannot prove whether the sum MI achieved by ⑤ is smaller or larger compared with ④, as this also depends highly on the realization of $\mathbf{H}$ and $\mathbf{G}$. Similarly, although we can prove that the sum MI of ⑧ is smaller than ⑥, it is not sure whether the MI of ⑧ is smaller than ⑦. Such uncertainties are marked by dashed lines in Fig. 2. In this regard, ⑤ and ⑧ may become local peaks of the sum MI.

The analysis above is very useful when we study the subchannel allocation under QoS constraints later in Section IV.

C. Power Allocation Algorithm

With a given subchannel allocation $\mathcal{I}$ and $\mathcal{J}$, the problem (31)-(36) becomes the following power allocation problem

$$\max_{\mathbf{x},\mathbf{y},\mathbf{z}} \sum_{i=1}^{N_1} \log_2\left(1+\frac{a_i x_i b_{\mathcal{I}_i} y_i}{1+a_i x_i+b_{\mathcal{I}_i} y_i}\right)+\sum_{j=1}^{N_2} \log_2(1+b_{\mathcal{J}_j} z_j) \quad (38)$$

$$\text{s.t.} \sum_{i=1}^{N_1} x_i \le P_s \quad (39)$$

$$\sum_{i=1}^{N_1} y_i + \sum_{j=1}^{N_2} z_j \le P_r \quad (40)$$

$$x_i > 0, \quad y_i > 0, \quad i = 1, \cdots, N_1 \quad (41)$$

$$z_j > 0, \quad j = 1, \cdots, N_2. \quad (42)$$

Note that for the optimal subchannel allocation in Theorem 2, we have $b_{\mathcal{I}_i} = b_{N_2+i}$, $i = 1, \cdots, N_1$ and $b_{\mathcal{J}_j} = b_j$, $j = 1, \cdots, N_2$. The problem (38)-(42) is nonconvex due to the first summation term in (38). In this subsection, we develop an efficient method to solve the problem (38)-(42) based on the primal decomposition technique [25].

By introducing $\sum_{i=1}^{N_1} y_i \le P_y$, the problem (38)-(42) can be decomposed into two subproblems. One subproblem focuses on the optimization of $\mathbf{x}$ and $\mathbf{y}$ as

$$\max_{\mathbf{x},\mathbf{y}} \sum_{i=1}^{N_1} \log_2\left(1+\frac{a_i x_i b_{\mathcal{I}_i} y_i}{1+a_i x_i+b_{\mathcal{I}_i} y_i}\right) \quad (43)$$

$$\text{s.t.} \sum_{i=1}^{N_1} x_i \le P_s, \quad x_i > 0,\ i = 1, \cdots, N_1 \quad (44)$$

$$\sum_{i=1}^{N_1} y_i \le P_y, \quad y_i > 0,\ i = 1, \cdots, N_1. \quad (45)$$

And the other subproblem optimizes $\mathbf{z}$ as

$$\max_{\mathbf{z}} \sum_{j=1}^{N_2} \log_2(1 + b_{\mathcal{J}_j} z_j) \quad (46)$$

$$\text{s.t.} \sum_{j=1}^{N_2} z_j \le P_r - P_y, \quad z_j > 0,\ j = 1, \cdots, N_2. \quad (47)$$

Let us denote $J_1(P_y)$ as the optimal value of (43), subjecting to constraints (44) and (45) with a given P_y. Similarly, we introduce $J_2(P_y)$ as the maximal value of the problem (46)-(47) for a fixed P_y. The master problem can be written as

$$\max_{P_y} \ J(P_y) \quad \text{s.t. } 0 \le P_y \le P_r \quad (48)$$

where $J(P_y) = J_1(P_y) + J_2(P_y)$. In fact, $J_1(P_y)$, $J_2(P_y)$, and $J(P_y)$ are the MI of the $\mathbf{s}_s$ link, the MI of the $\mathbf{s}_r$ link, and the sum MI, respectively.

Theorem 3: $J(P_y)$ is a concave function of P_y in $[0, P_r]$ with any given $\mathbf{x}$ satisfying (44).

Proof: See Appendix C. ■

Theorem 3 indicates that $J(P_y)$ is a unimodal function. The unimodality of $J(P_y)$ is also clearly shown in Fig. 3 for a system with $N_s = 3$, $N_r = 5$, $N_d = 5$, $N_1 = 3$, $N_2 = 2$, and $\mathrm{SNR}_s = \mathrm{SNR}_r = 20$ dB. Thus, the optimal P_y in the master problem (48) can be efficiently obtained through a one dimensional search. In this paper, we employ the golden section search method [28] to obtain the optimal P_y. For a given P_y, the subproblem (43)-(45) can be solved by using the alternating water-filling approach in [10], and the subproblem (46)-(47) has the classical water-filling solution [29]. Based on this analysis, the problem (38)-(42) can be efficiently solved by following the primal decomposition based approach in Algorithm 1, where $(\cdot)^*$ denotes the optimal value, ε is a small positive threshold close to 0, and $\beta = (3-\sqrt{5})/2$

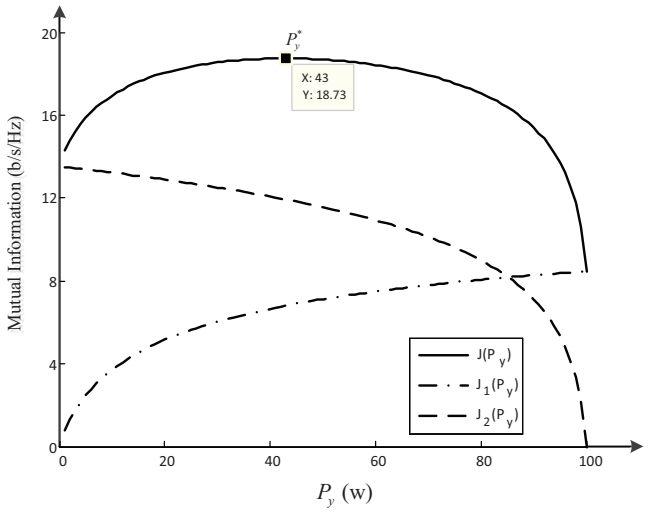

Fig. 3. MI versus P_y. $N_s = 3$, $N_r = 5$, $N_d = 5$, $N_1 = 3$, $N_2 = 2$, and $\mathrm{SNR}_s = \mathrm{SNR}_r = 20$ dB.

is known as the golden ratio. We would like to note that in general, Theorem 2 and the primal decomposition technique cannot be directly applied to other Schur-concave objective functions.

Algorithm 1 Solving the Problem (38)-(42) Based on the Primal Decomposition Approach

Input: P_s, P_r, a_i, $i = 1, \cdots, N_1$, and b_k, $k = 1, \cdots, N$.
Output: $\mathbf{x}^*$, $\mathbf{y}^*$, $\mathbf{z}^*$, P_y^*, $J_1(P_y^*)$, $J_2(P_y^*)$, and $J(P_y^*)$.
Initialize the lower bound p_l and the upper bound p_u of P_y as $p_l = 0$ and $p_u = P_r$.
while $p_u - p_l > \varepsilon$ **do**
  Define $v_1 = (1-\beta)p_l + \beta p_u$ and $v_2 = \beta p_l + (1-\beta)p_u$.
  Solve the problem (43)-(45) and the problem (46)-(47) for $P_y = v_1$ to obtain $J_1(v_1)$ and $J_2(v_1)$. Compute $J(v_1) = J_1(v_1) + J_2(v_1)$.
  Repeat Step 3 for $P_y = v_2$.
  if $J(v_1) < J(v_2)$ **then**
    Assign $p_l = v_1$.
  else
    Assign $p_u = v_2$.
  end if
end while
Let $P_y^* = (p_u + p_l)/2$. Calculate $\mathbf{x}^*$, $\mathbf{y}^*$, and $J_1(P_y^*)$ by solving the problem (43)-(45).
Obtain $\mathbf{z}^*$ and $J_2(P_y^*)$ by solving the problem (46)-(47). Calculate $J(P_y^*) = J_1(P_y^*) + J_2(P_y^*)$.

IV. QoS Constraints

It can be seen from Theorem 2 that the maximal sum MI criterion might lead to fairness issues, as the source signals $\mathbf{s}_s$ are assigned with weaker second-hop subchannels compared with those allocated to the relay signals $\mathbf{s}_r$. To solve this problem, we impose additional QoS constraints in terms of the lower bounds of the MI of each link. Using the maximal MI criterion and considering the rate constraints, the joint subchannel and power allocation problem becomes

$$\max_{\mathcal{I},\mathcal{J},\mathbf{x},\mathbf{y},\mathbf{z}} \sum_{i=1}^{N_1} \log_2\left(1+\frac{a_i x_i b_{\mathcal{I}_i} y_i}{1+a_i x_i + b_{\mathcal{I}_i} y_i}\right) + \sum_{j=1}^{N_2} \log_2(1+b_{\mathcal{J}_j} z_j) \quad (49)$$

$$\text{s.t.} \sum_{i=1}^{N_1} x_i \le P_s \quad (50)$$

$$\sum_{i=1}^{N_1} y_i + \sum_{j=1}^{N_2} z_j \le P_r \quad (51)$$

$$\sum_{i=1}^{N_1} \log_2\left(1+\frac{a_i x_i b_{\mathcal{I}_i} y_i}{1+a_i x_i + b_{\mathcal{I}_i} y_i}\right) \ge r_1 \quad (52)$$

$$\sum_{j=1}^{N_2} \log_2(1+b_{\mathcal{J}_j} z_j) \ge r_2 \quad (53)$$

$$x_i > 0, \quad y_i > 0, \quad i = 1, \cdots, N_1 \quad (54)$$

$$z_j > 0, \quad j = 1, \cdots, N_2 \quad (55)$$

$$\underline{\mathcal{I}} = N_1, \underline{\mathcal{J}} = N_2, \mathcal{I} \cap \mathcal{J} = \emptyset, \mathcal{I} \cup \mathcal{J} = \{1, \cdots, N\} \quad (56)$$

where r_1 and r_2 are the minimal rate requirement of transmitting $\mathbf{s}_s$ and $\mathbf{s}_r$, respectively. Compared with the problem (31)-(36), the problem (49)-(56) is much more challenging to solve due to the constraints (52) and (53). Obviously, because of the additional constraints (52) and (53), the maximal value of (49) may be smaller than that of (31).

A. Subchannel Allocation

Due to the inclusion of the constraints (52) and (53), the subchannel allocation scheme proposed in Theorem 2 may be suboptimal for the problem (49)-(56), or may even fail to satisfy the QoS constraints (52) and (53). In fact, the optimal subchannel allocation highly depends on the value of r_1 and r_2.

As a combinatorial problem, the optimal subchannel allocation for the problem (49)-(56) can be obtained through an exhaustive search over all possible combinations of $\mathcal{I}$ and $\mathcal{J}$ satisfying (56), and choose the best one with a maximal value of (49). However, this method has a prohibitively high computational complexity, especially when N_1 and N_2 are large. To reduce the computational complexity, in this subsection, we propose a suboptimal subchannel allocation method with a low complexity.

It can be seen from Fig. 2 that there are locally optimal subchannel allocations (e.g., peaks ①, ⑤, and ⑧). Base on the analysis in Section III-B, we can see that the sum MI of the local peaks exhibits a decreasing trend with the increase of the combination number (i.e., ①>⑤>⑧). Inspired by this observation, the key idea of the proposed scheme is that instead of searching over all combinations of $\mathcal{I}$ and $\mathcal{J}$, we study the subchannel allocations in an increasing order of n starting from $n = 1$ (see Fig. 2), and the search stops when the first peak is found. The rationale and the details of the proposed scheme are explained below.

Let us introduce

$$f_1^{(n)}(\mathbf{x},\mathbf{y}) = \sum_{i=1}^{N_1} \log_2\left(1+\frac{a_i x_i b_{\mathcal{I}_i}^{(n)} y_i}{1+a_i x_i + b_{\mathcal{I}_i}^{(n)} y_i}\right)$$

$$f_2^{(n)}(\mathbf{z}) = \sum_{j=1}^{N_2} \log_2(1+b_{\mathcal{J}_j}^{(n)} z_j)$$

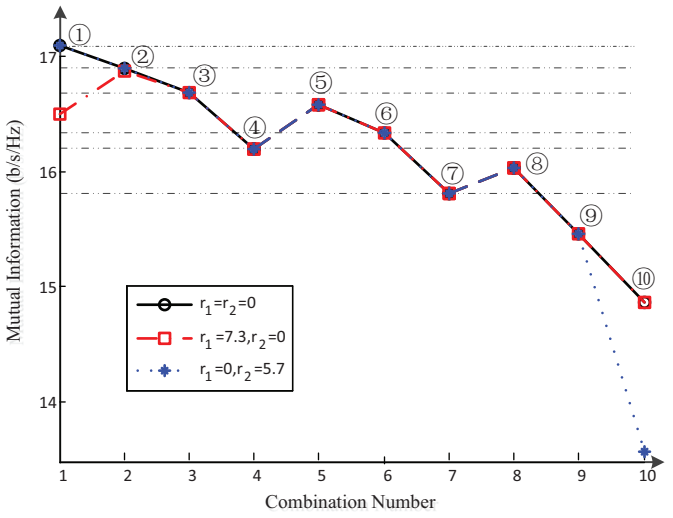

Fig. 4. The impact of QoS constraints on the subchannel allocation schemes. $N_s = 3$, $N_r = 5$, $N_d = 5$, $N_1 = 3$, $N_2 = 2$, and $\text{SNR}_s = \text{SNR}_r = 20$ dB.

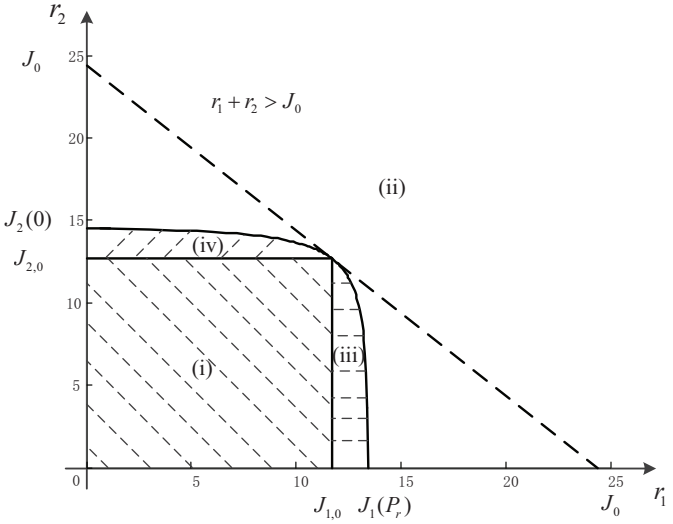

Fig. 5. The feasible region of r_1 and r_2. $N_s = 3$, $N_r = 5$, $N_d = 5$, $N_1 = 3$, $N_2 = 2$, and $\text{SNR}_s = \text{SNR}_r = 20$ dB.

as the MI for the $\mathbf{s}_s$ and $\mathbf{s}_r$ links, respectively, where the superscript (n) denotes the value at the n-th subchannel allocation. Let $f_1^{(n)*}$ and $f_2^{(n)*}$ denote the values of $f_1^{(n)}(\mathbf{x}, \mathbf{y})$ and $f_2^{(n)}(\mathbf{z})$, respectively, obtained from solving the problem (38)-(42) under the n-th subchannel allocation. It can be seen from (37) that from ① to ⑩, the gains of subchannels in $\mathcal{A}$ are in a decreasing order, while those in $\mathcal{B}$ are in an increasing order. Thus, $f_2^{(n)*}$ has a similar decreasing trend with respect to n as the sum MI in Fig. 2, while in general the value of $f_1^{(n)*}$ increases with respect to n.

Now we study the scenario where r_1 increases with a fixed r_2 ($r_2 \leq f_2^{(n)*}$). When $r_1 \leq f_1^{(n)*}$, constraints (52) and (53) are not tight. Obviously, the solution of the problem (49)-(56) is identical to that of the problem (31)-(36) in this case. Thus, the subchannel allocation in Theorem 2 (first peak ① with $r_1 = r_2 = 0$ in Fig. 4) is optimal. When $r_1 > f_1^{(n)*}$, the constraint (52) is not redundant any more. As a result, the maximal value of (49) at the n-th combination is smaller compared with that of (31). When $r_1 + r_2 > f_1^{(n)*} + f_2^{(n)*}$, the n-th subchannel allocation becomes infeasible.

According to the analysis above, the value of $f_1^{(n)*}$ increases with respect to n in general. Therefore, the reduction of the objective function (49) due to the constraint (52) diminishes with increasing n. This fact is illustrated in Fig. 4 with $r_1 = 7.3$ b/s/Hz and $r_2 = 0$, where it can be seen that the sum MI is only affected by subchannel allocations associated with a smaller n, while those with a larger n are not affected by (52). It can also be observed from Fig. 4 that the local peaks still present a decreasing trend with respect to n. Thus, we can take the allocation n associated with the first peak as the best subchannel allocation.

Now we investigate the case that r_2 increases with a fixed r_1 ($r_1 \leq f_1^{(n)*}$). Similarly, it can be easily seen that the reduction of the objective function (49) due to the constraint (53) increases with n as shown in Fig. 4 ($r_1 = 0$ and $r_2 = 5.7$ b/s/Hz). Thus, in this case, the subchannel allocation in Theorem 2 (first peak ① in Fig. 4) is optimal. Combining the analysis in the two cases above, we propose a channel allocation strategy which starts searching from $n = 1$ and continues searching till the first peak of the sum MI is found.

We would like to note that when N_1 and N_2 increase, there are more uncertainties in the sum MI versus n like that between ④ and ⑤ in Fig. 4. Although the local peaks have a decreasing trend with respect to n in the case of small r_1, there may be opposite trend in several local peaks when r_1 is large. In this case, the proposed subchannel allocation scheme might be suboptimal. It will be shown in Section V that compared with the exhaustive search based subchannel allocation scheme, the proposed algorithm has only a small performance loss, but with a much lower computational complexity.

B. Power Allocation

With a fixed subchannel allocation $\mathcal{I}$ and $\mathcal{J}$, the problem (49)-(56) becomes the power allocation problem below

$$\max_{\mathbf{x},\mathbf{y},\mathbf{z}} \sum_{i=1}^{N_1} \log_2\left(1+\frac{a_i x_i b_{\mathcal{I}_i} y_i}{1+a_i x_i+b_{\mathcal{I}_i} y_i}\right)+\sum_{j=1}^{N_2} \log_2(1+b_{\mathcal{J}_j} z_j) \quad (57)$$

$$\text{s.t.} \sum_{i=1}^{N_1} x_i \leq P_s \quad (58)$$

$$\sum_{i=1}^{N_1} y_i + \sum_{j=1}^{N_2} z_j \leq P_r \quad (59)$$

$$\sum_{i=1}^{N_1} \log_2\left(1 + \frac{a_i x_i b_{\mathcal{I}_i} y_i}{1 + a_i x_i + b_{\mathcal{I}_i} y_i}\right) \geq r_1 \quad (60)$$

$$\sum_{j=1}^{N_2} \log_2(1 + b_{\mathcal{J}_j} z_j) \geq r_2 \quad (61)$$

$$x_i > 0, \quad y_i > 0, \quad i = 1, \cdots, N_1 \quad (62)$$

$$z_j > 0, \quad j = 1, \cdots, N_2. \quad (63)$$

In this subsection, we develop a new algorithm to efficiently solve the problem (57)-(63) by exploiting the results in Sec-

tion III-C.

The feasible region (r_1, r_2) of the problem (57)-(63) is shown in Fig. 5 under a typical realization of $\mathbf{H}$ and $\mathbf{G}$ with $N_s = 3$, $N_r = 5$, $N_d = 5$, $N_1 = 3$, $N_2 = 2$, and $\mathrm{SNR}_s = \mathrm{SNR}_r = 20$ dB. As a starting point, we solve the problem (38)-(42) using Algorithm 1 and denote the output as $\mathbf{x}_0$, $\mathbf{y}_0$, $\mathbf{z}_0$, $P_{y,0}$, $J_{1,0}$, $J_{2,0}$, and J_0. Firstly, if $r_1 \leq J_{1,0}$ and $r_2 \leq J_{2,0}$, the rate constraints (60) and (61) are satisfied. This corresponds to Region (i) in Fig. 5. In this case, the solution of the problem (38)-(42) is the solutions to the problem (57)-(63).

Secondly, due to the additional constraints (60) and (61), the maximal value of the objective function (57) is smaller than or equal to that in (38). Thus, if $r_1 + r_2 > J_0$, the problem (57)-(63) is infeasible. Moreover, it can be seen from the problem (43)-(45) that the maximal value of (43) is achieved at $P_y = P_r$. Thus, the maximal feasible r_1 is $J_1(P_r)$. Similarly, we can see from the problem (46)-(47) that the maximum of (46) is attained when $P_y = 0$. Therefore, the maximal feasible r_2 is $J_2(0)$. The infeasible combinations of (r_1, r_2) are shown in Region (iv) in Fig. 5.

Algorithm 2 Solving the Problem (57)-(63) Based on Algorithm 1

Input: P_s, P_r, r_1, r_2, a_i, $i = 1, \cdots, N_1$, and b_k, $k = 1, \cdots, N$.
Output: $\mathbf{x}^*$, $\mathbf{y}^*$, $\mathbf{z}^*$, and $J(P_y^*)$.

```
Run Algorithm 1 and denote the output of Algorithm 1 as x_0, y_0, z_0, P_{y,0}, J_{1,0}, J_{2,0}, and J_0.
Obtain J_1(P_r) by solving the problem (43)-(45) with P_y = P_r.
Calculate J_2(0) by solving the problem (46)-(47) with P_y = 0.
if r_1 ≤ J_{1,0} and r_2 ≤ J_{2,0} then
    return x* = x_0, y* = y_0, z* = z_0, and J(P_y^*) = J_0.
else if r_1 + r_2 > J_0, or r_1 > J_1(P_r), or r_2 > J_2(0) then
    return Problem infeasible.
else if J_{1,0} < r_1 ≤ J_1(P_r) then
    Find P_{y,r_1}, x*, and y* such that J_1(P_{y,r_1}) = r_1 from solving the problem (43)-(45).
    Solve the problem (46)-(47) with P_{y,r_1} and obtain z* and J_2(P_{y,r_1}).
    if r_2 > J_2(P_{y,r_1}) then
        return Problem infeasible.
    else
        return x*, y*, z*, and J(P_y^*) = J(P_{y,r_1}).
    end if
else
    Find P_{y,r_2} and z* such that J_2(P_{y,r_2}) = r_2 from solving the problem (46)-(47).
    Solve the problem (43)-(45) with P_{y,r_2} and obtain x*, y*, and J_1(P_{y,r_2}).
    if r_1 > J_1(P_{y,r_2}) then
        return Problem infeasible.
    else
        return x*, y*, z*, and J(P_y^*) = J(P_{y,r_2}).
    end if
end if
```

Thirdly, when $J_{1,0} < r_1 \leq J_1(P_r)$, $J_{1,0}$ cannot satisfy the rate constraint (60). Thus, we need to increase P_y over $P_{y,0}$ such that $J_1(P_y)$ can be increased to satisfy (60). On the other hand, it can be seen from Fig. 3 that $J(P_y)$ decreases with P_y for $P_y > P_y^*$ (i.e., $P_{y,0}$), which indicates that the increase of P_y relative to $P_{y,0}$ should be as small as possible. Therefore, the best P_y in this case is to just meet $J_1(P_y) = r_1$. We denote such P_y as P_{y,r_1}.

This P_{y,r_1} can be efficiently found by a bisection search [30] over the interval of $[P_{y,0}, P_r]$. For each attempt of P_y, we solve the problem (43)-(45) with this P_y, and check whether $J_1(P_y) = r_1$ is met and then adjust the search region according to the rule of bisection. After P_{y,r_1} is found, we solve the problem (46)-(47) to obtain $J_2(P_{y,r_1})$. If $r_2 > J_2(P_{y,r_1})$, the problem (57)-(63) is infeasible. Otherwise, the optimal value of (57) is $J(P_{y,r_1})$. The feasible (r_1, r_2) in this case is shown in Region (iii) in Fig. 5.

Lastly, for $J_{2,0} < r_2 \leq J_2(0)$. Similar to the analysis above, the best P_y is the solution of $J_2(P_y) = r_2$. We can obtain such P_y, denoted as P_{y,r_2}, through a bisection search over the interval of $[0, P_{y,0}]$. Then we solve the problem (43)-(45) to obtain $J_1(P_{y,r_2})$. If $r_1 < J_1(P_{y,r_2})$, the optimal value of (57) is $J(P_{y,r_2})$. Otherwise, the problem (57)-(63) is infeasible. Region (iv) in Fig. 5 illustrates the feasible (r_1, r_2) in this case.

In summary, the problem (57)-(63) can be solved based on which of the four regions (r_1, r_2) resides in. The proposed algorithm for solving the problem (57)-(63) is outlined in Algorithm 2. We would like to note that general nonlinear programming tools such as fmincon in Matlab can be employed to solve the problem (57)-(63). However, as will be shown in the simulations that the proposed algorithm has a much lower computational complexity than that of the fmincon tool.

V. Numerical Examples

In this section, we investigate the performance of the proposed algorithm through numerical simulations. In the simulations, we assume that the three nodes are located on a line where the distance between the source and destination nodes is fixed to $2L$ for all simulations. The source-relay and relay-destination distances are dL and $(2-d)L$, respectively, where $0 < d < 2$ is the normalized source-relay distance. We have $d = 1$ if the relay node is located in the middle of the source and destination nodes. The path loss exponent is $\eta = 3$. The entries of the source-relay matrix $\mathbf{H}$ and the relay-destination matrix $\mathbf{G}$ have complex Gaussian distribution with zero mean and variances of $1/(N_s(dL)^\eta)$ and $1/(N_r((2-d)L)^\eta)$, respectively. For the proposed approach, in the case of $r_1 = r_2 = 0$, Theorem 2 is applied for the subchannel allocation followed by Algorithm 1 for the power allocation. With $r_1, r_2 > 0$, the subchannel allocation scheme in Section IV-A is applied together with the power allocation algorithm in Algorithm 2. The SNRs of the first hop and the second hop channels are defined as $\mathrm{SNR}_s = P_s/(N_s(dL)^\eta)$ and $\mathrm{SNR}_r = P_r/(N_r((2-d)L)^\eta)$, respectively.

To the best of our knowledge, there is no other work in open literature which studied the transceiver optimization problem for the AF MIMO relay system in Fig. 1. Thus, we compare the proposed algorithm with the following three benchmarking approaches. In the first approach, exhaustive searching is employed to obtain the optimal subchannel allocation $\mathcal{I}$ and $\mathcal{J}$, and the Matlab tool 'fmincon' for constrained nonlinear programming is adopted to solve the power allocation problem (38)-(42) (in case of $r_1 = r_2 = 0$) or the problem (57)-(63) (for $r_1, r_2 > 0$). We denote this approach as 'exhaustive+fmincon'. In the second approach, exhaustive searching

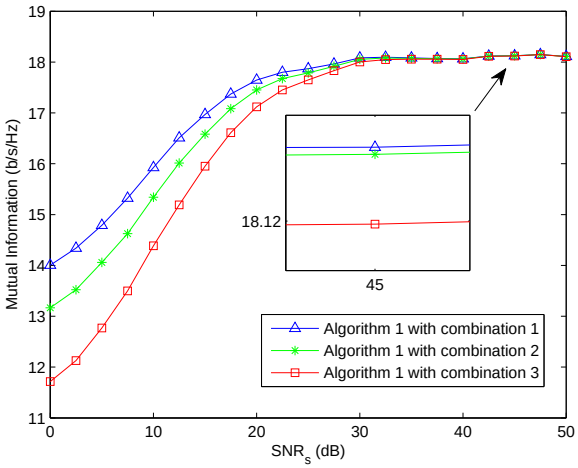

Fig. 6. Example 1: MI versus SNR_s. $N_s = 3$, $N_r = 5$, $N_d = 5$, $N_1 = 3$, $N_2 = 2$, $d = 1$, $r_1 = r_2 = 0$, and $\mathrm{SNR}_r = 20$ dB.

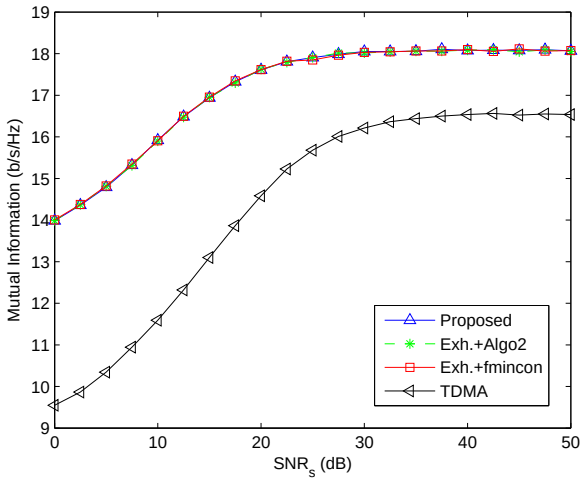

Fig. 7. Example 2: MI versus SNR_s. $N_s = 3$, $N_r = 5$, $N_d = 5$, $N_1 = 3$, $N_2 = 2$, $d = 1$, $r_1 = r_2 = 0.5$ b/s/Hz, and $\mathrm{SNR}_r = 20$ dB.

is used for the subchannel allocation, and Algorithms 1 or 2 is adopted for power allocation. For simplicity, the second approach is denoted as 'exhaustive+Algo$i$', where i is 1 or 2. In the third approach, a simple time-division multiple access (TDMA) method with 3-phase time slots is applied for the AF MIMO relay system in Fig. 1. In particular, during the first two time slots, the source node sends information to the destination node via the relay node, and then at the third time slot, the relay node transmits its own information to the destination node. Since the TDMA method completes the communication process in three time slots, a factor of $2/3$ needs to be considered when comparing the sum MI of the TDMA system with that of the proposed system. Unless stated otherwise, the MI results in the simulations refer to the sum MI of both the $\mathbf{s}_s$ and $\mathbf{s}_r$ links. All simulation results are averaged through 1000 Monte-Carlo runs.

In the first simulation example, we study the performance of Algorithm 1 when $r_1 = r_2 = 0$. We set $N_s = 3, N_r = 5, N_d = 5, N_1 = 3$, $N_2 = 2$, $d = 1$, and $\mathrm{SNR}_r = 20$ dB. Fig. 6 shows the system MI yielded by Algorithm 1 versus SNR_s with the subchannel allocations ①, ②, and ③ in (37). It can be seen from Fig. 6 that when SNR_s increases from 0 dB to 35 dB, the system MI by all three subchannel allocation schemes increases. When $\mathrm{SNR}_s > 35$ dB, the system MI of all three allocation schemes remains almost unchanged. Such an MI ceiling is caused by the limited power at the relay node, which will also be observed in the following numerical examples. We also observe from Fig. 6 that the subchannel allocation ① achieves the largest MI among all three schemes throughout the whole SNR_s range, which corroborates Theorem 2. Interestingly, the MI gaps among three channel allocation schemes diminish as SNR_s increases.

In the second example, we consider the QoS constraints where $r_1 = r_2 = 0.5$ b/s/Hz and we set $N_s = 3, N_r = 5, N_d = 5, N_1 = 3$, $N_2 = 2$, and $d = 1$. Fig. 7 shows the MI of the four algorithms versus SNR_s when $\mathrm{SNR}_r = 20$ dB. We can observe from Fig. 7 that the proposed algorithm,

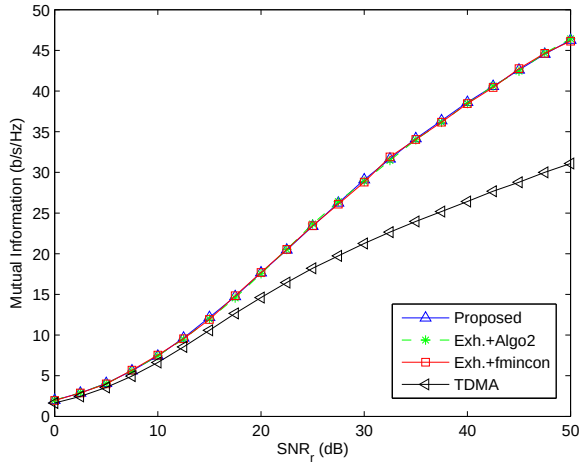

Fig. 8. Example 2: MI versus SNR_r. $N_s = 3$, $N_r = 5$, $N_d = 5$, $N_1 = 3$, $N_2 = 2$, $d = 1$, $r_1 = r_2 = 0.5$ b/s/Hz, and $\mathrm{SNR}_s = 20$ dB.

the exhaustive+fmincon algorithm, and the exhaustive+Algo2 approach almost yield the same system MI at the whole range of SNR_s. In particular, when $\mathrm{SNR}_s < 25$ dB, the MI of the three algorithms increases with SNR_s. And the system MI reaches a ceiling when $\mathrm{SNR}_s > 25$ dB. We can also see from Fig. 7 that due to the $2/3$ scaling factor, the TDMA system has the smallest system MI over the whole SNR_s range.

For this example, the system MI of the four algorithms versus SNR_r when $\mathrm{SNR}_s = 20$ dB is illustrated in Fig. 8. It can be seen from Fig. 8 that the proposed algorithm, the exhaustive+fmincon algorithm, and the exhaustive+Algo2 approach yield almost identical MI and they have a better MI performance than the TDMA method throughout the SNR_r region. However, different to Fig. 7, the achievable MI of the four algorithms increases at the whole range of SNR_r. Moreover, the MI gap between the TDMA method and the other three algorithms increases with SNR_r.

In the third example, we investigate the impact of r_1 and

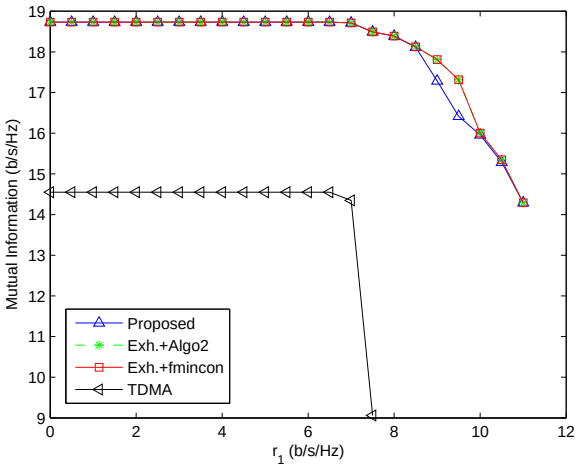

Fig. 9. Example 3: MI versus r_1 with fixed $\mathbf{H}$ and $\mathbf{G}$. $N_s = 3$, $N_r = 5$, $N_d = 5$, $N_1 = 3$, $N_2 = 2$, $d = 1$, $r_2 = 0.5$ b/s/Hz, and $\text{SNR}_s = \text{SNR}_r = 20$ dB.

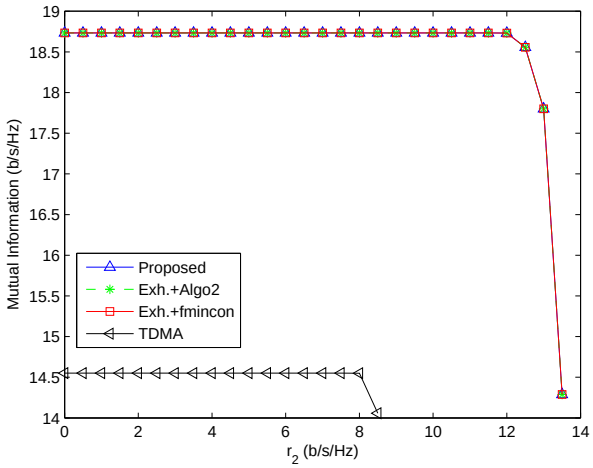

Fig. 10. Example 3: MI versus r_2 with fixed $\mathbf{H}$ and $\mathbf{G}$. $N_s = 3$, $N_r = 5$, $N_d = 5$, $N_1 = 3$, $N_2 = 2$, $d = 1$, $r_1 = 0.5$ b/s/Hz, and $\text{SNR}_s = \text{SNR}_r = 20$ dB.

r_2 on the proposed algorithm. We fix the channel matrices $\mathbf{H}$ and $\mathbf{G}$ and set $N_s = 3$, $N_r = 5$, $N_d = 5$, $N_1 = 3$, $N_2 = 2$, $d = 1$, and $\text{SNR}_s = \text{SNR}_r = 20$ dB. Fig. 9 shows the MI comparison of the four algorithms versus r_1 at $r_2 = 0.5$ b/s/Hz. From Fig. 9, we find that for the proposed algorithm, the exhaustive+fmincon algorithm, and the exhaustive+Algo2 approach, the achievable system sum MI does not change for $r_1 \leq 7$ b/s/Hz as the rate constraint (52) is not active for these r_1. When $r_1 > 7$ b/s/Hz, the constraint (52) becomes active, and thus, the sum MI decreases with an increasing r_1 in order to satisfy (52). Moreover, we also observe from Fig. 9 that the exhaustive+Algo2 approach achieves the same MI as the exhaustive+fmincon algorithm, which indicates that Algorithm 2 has a similar MI performance as the fmincon algorithm. However, it will be shown later that Algorithm 2 has a lower computational complexity than the fmincon algorithm. This shows that Algorithm 2 is more suitable for practical AF MIMO relay systems.

It can also be seen from Fig. 9 that the proposed algorithm achieves the same MI as the exhaustive+fmincon algorithm and the exhaustive+Algo2 approach when $r_1 \leq 8.5$ b/s/Hz, and the former algorithm performs a little worse than the latter two when $r_1 > 8.5$ b/s/Hz. This is expected based on the analysis in Section IV-A, where it is mentioned that the proposed subchannel allocation scheme is suboptimal in the case of large r_1. However, it will be shown later that the proposed subchannel allocation scheme has a much lower computational complexity than the exhaustive search algorithm. We can also observe from Fig. 9 that the TDMA method yields the lowest system MI at various values of r_1. Interestingly, in the TDMA method, the rate constraint of the $\mathbf{s}_s$ link is not active until $r_1 = 7$ b/s/Hz. When $r_1 > 7.5$ b/s/Hz, the TDMA method fails to find the solution.

For this example, the MI of the four algorithms versus r_2 at $r_1 = 0.5$ b/s/Hz is shown in Fig. 10. It can be seen from Fig. 10 that the proposed algorithm, the exhaustive+fmincon algorithm, and the exhaustive+Algo2 approach exhibit the same MI performance throughout the whole range of r_2, which corroborates the analysis in Section IV-A. In particular, for $r_2 \leq 12$ b/s/Hz, the achievable system sum MI of these three algorithms does not change as the rate constraint (53) is not active for these r_2. For $r_2 > 12$ b/s/Hz, the constraint (53) becomes active, and thus the system MI decreases with increasing r_2, in order to satisfy (53). Moreover, the system MI of the TDMA method is lower than that of the other three algorithms. Interestingly, different to the other three algorithms, the MI of the TDMA method does not change until $r_2 = 8$ b/s/Hz and the solution cannot be found for the TDMA method when $r_2 > 8.5$ b/s/Hz.

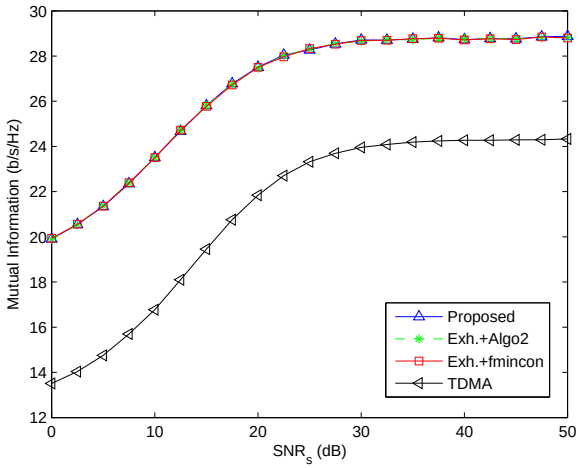

Fig. 11. Example 4: MI versus SNR_s. $N_s = 8$, $N_r = 10$, $N_d = 10$, $N_1 = 5$, $N_2 = 3$, $d = 1$, $r_1 = r_2 = 0.5$ b/s/Hz, and $\text{SNR}_r = 20$ dB.

In the next example, we study the MI performance of the proposed algorithm when the AF MIMO relay system has a larger dimension. In particular, we set $N_s = 8$, $N_r = 10$, $N_d = 10$, $N_1 = 5$, $N_2 = 3$, $d = 1$, and $r_1 = r_2 = 0.5$ b/s/Hz. Fig. 11 shows the MI of the four algorithms versus SNR_s when $\text{SNR}_r = 20$ dB. It can be seen that the four curves in

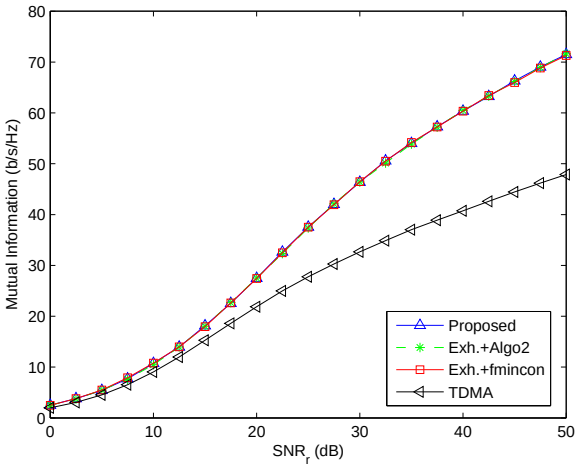

Fig. 12. Example 4: MI versus SNR_r. $N_s = 8$, $N_r = 10$, $N_d = 10$, $N_1 = 5$, $N_2 = 3$, $d = 1$, $r_1 = r_2 = 0.5$ b/s/Hz, and $\mathrm{SNR}_s = 20$ dB.

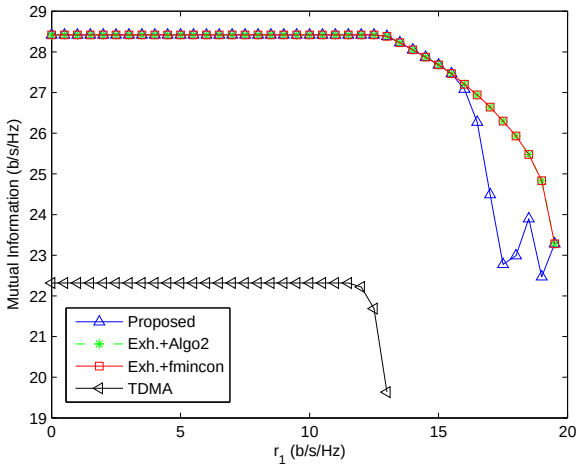

Fig. 13. Example 5: MI versus r_1 with fixed $\mathbf{H}$ and $\mathbf{G}$. $N_s = 8$, $N_r = 10$, $N_d = 10$, $N_1 = 5$, $N_2 = 3$, $d = 1$, $r_2 = 0.5$ b/s/Hz, and $\mathrm{SNR}_s = \mathrm{SNR}_r = 20$ dB.

Fig. 11 display a similar trend to those in Fig. 7. Moreover, by comparing Fig. 11 with Fig. 7, we can observe that when N_1 and N_2 increase, the system MI of the four algorithms increase and the MI gap between the TDMA method and the other three algorithms widens.

The system MI achieved by the four algorithms versus SNR_r at $\mathrm{SNR}_s = 20$ dB is shown in Fig. 12. We can observe from Fig. 12 that similar to Fig. 8, the system MI of the four algorithms increases with SNR_r and the TDMA method performs worse than the other three algorithms throughout the whole SNR_r range. Figs. 11 and 12 clearly demonstrate that the proposed algorithm works efficiently also in AF MIMO relay systems with a larger dimension.

In the fifth simulation example, we investigate the MI performance of the proposed algorithm at various r_1 and r_2. We fix $\mathbf{H}$ and $\mathbf{G}$ and choose $N_s = 8$, $N_r = 10$, $N_d = 10$, $N_1 = 5$, $N_2 = 3$, $d = 1$, and $\mathrm{SNR}_s = \mathrm{SNR}_r = 20$ dB. In Fig. 13, we illustrate the MI of the four algorithms versus r_1 when $r_2 = 0.5$ b/s/Hz. It can be seen from Fig. 13 that for the proposed algorithm, the exhaustive+fmincon algorithm, and the exhaustive+Algo2 approach, the system sum MI remains same till $r_1 = 13$ b/s/Hz and after that, the system MI decreases with increasing r_1. Moreover, these three algorithms yield the same MI when $r_1 \leq 15.5$ b/s/Hz. When $r_1 > 15.5$ b/s/Hz, the system MI of the proposed algorithm is smaller than that of the exhaustive searching-based approaches. Different to Fig. 9, the system sum MI achieved by the proposed algorithm fluctuates when r_1 is large. This is caused by the local optimality of the proposed algorithm at large N_1 and N_2 as stated in Section IV-A. The TDMA method has a worse MI performance than the other three algorithms with an active rate constraint of the $\mathbf{s}_s$ link after $r_1 = 11.5$ b/s/Hz and fails to find the solution after $r_1 = 13$ b/s/Hz.

The MI of the four algorithms versus r_2 when $r_1 = 0.5$ b/s/Hz is shown in Fig. 14. It can be observed from Fig. 14 that similar to Fig. 10, the proposed algorithm, the exhaustive+fmincon algorithm, and the exhaustive+Algo2 approach have the same MI performance which is better than that of

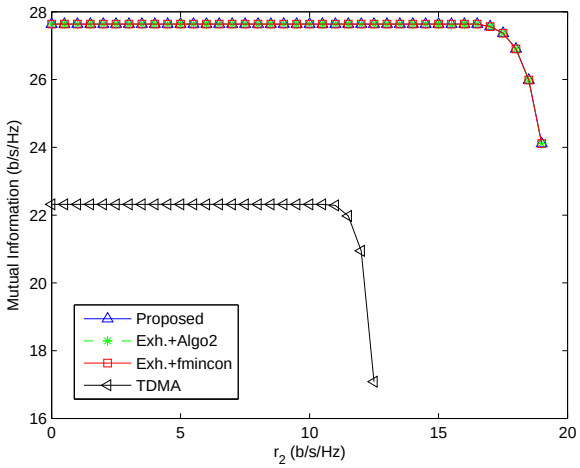

Fig. 14. Example 5: MI versus r_2 with fixed $\mathbf{H}$ and $\mathbf{G}$. $N_s = 8$, $N_r = 10$, $N_d = 10$, $N_1 = 5$, $N_2 = 3$, $d = 1$, $r_1 = 0.5$ b/s/Hz, and $\mathrm{SNR}_s = \mathrm{SNR}_r = 20$ dB.

the TDMA method for the whole range of r_2. Moreover, the system MI of the former three methods remains unchanged till $r_2 = 17$ b/s/Hz and then decreases with increasing r_2. The TDMA method has the same system MI till $r_2 = 11$ b/s/Hz and fails to solve the problem after $r_2 = 12.5$ b/s/Hz.

In the sixth example, we study the impact of relay positions on the system sum MI. We set $N_s = N_r = N_d = 8$, $N_1 = N_2 = 4$, $r_1 = 5.5$ b/s/Hz, and $r_2 = 6.5$ b/s/Hz. Fig. 15 shows the system sum MI achieved by the four algorithms versus d. We can see from Fig. 15 that the MI of the four algorithms increases with d. The TDMA method has a worse MI performance than the other three algorithms and the MI gap widens when d increases. The reasons are explained below. As d increases, the gain of the source-relay channels a_i, $i = 1, \cdots, N_1$ decreases, while the gain of the relay-destination links b_k, $k = 1, \cdots, N$ increases. Thus, the MI for the signals from the relay node (MIR) increases with

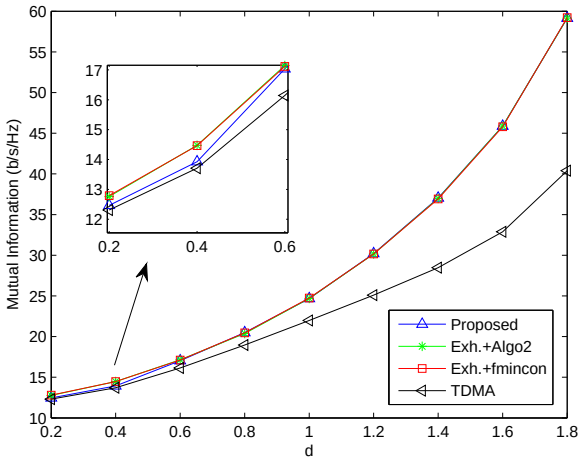

Fig. 15. Example 6: MI versus d. $N_s = N_r = N_d = 8$, $N_1 = N_2 = 4$, $r_1 = 5.5$ b/s/Hz, and $r_2 = 6.5$ b/s/Hz.

TABLE I
THE COMPUTATION TIME VERSUS N_1, $r_1 = r_2 = 0.5$ b/s/Hz.

N_1	1	2	3	4	5	6
Proposed	**0.07**	**0.32**	**0.40**	**0.48**	**0.65**	**0.81**
Exhaustive+Algo2	0.07	1.73	4.33	8.93	18.47	34.03
Exhaustive+fmincon	0.51	2.02	5.53	12.93	26.12	48.66

d. For the TDMA method, the MI for the signals from the source node (MIS) first increases and then decreases with an increasing d. Fig. 15 indicates that when MIS decreases with d, the amount of reduction is smaller than the amount of increase in MIR. For the other three algorithms, both the MIS and MIR increase with d. This leads to an increased sum MI gap between the proposed system and the TDMA method. We can also observe from Fig. 15 that the proposed algorithm, the exhaustive+fmincon algorithm, and the exhaustive+Algo2 approach exhibit the same MI performance when $d \geq 0.6$ and the proposed algorithm performs a little worse than the exhaustive searching-based approaches when $d < 0.6$.

Lastly, we look into the computational cost of the proposed algorithm. We choose an AF MIMO relay system with $N_s = N_r = N_d = 10$, $N_2 = 3$, $d = 1$, and $\text{SNR}_s = \text{SNR}_r = 20$ dB. Table I shows the computation time in seconds required by the proposed algorithm, the exhaustive+fmincon algorithm, and the exhaustive+Algo2 approach at various N_1 with $r_1 = r_2 = 0.5$ b/s/Hz. It can be seen from Table I that the computation time required by all three algorithms increases with N_1, as the number of optimization variables increases with N_1. Moreover, we can observe that the exhaustive+Algo2 approach needs shorter time than the exhaustive+fmincon algorithm, which indicates that Algorithm 2 is more computationally efficient than the fmincon tool. Furthermore, the proposed algorithm requires much shorter computation time compared with the other two algorithms, particularly for large N_1. This proves that the subchannel allocation algorithm in Section IV-A is much more efficient than the exhaustive search approach.

The computation time of the three algorithms with $r_1 = 8$ b/s/Hz and $r_2 = 10$ b/s/Hz at various N_1 is shown in Table II. By comparing Table I with Table II, we find that the computation time of all three algorithms increases in general when r_1 and r_2 increase, which makes the constraints (52) and (53) stricter. Similar to Table I, we can observe from Table II that among the three algorithms, the proposed algorithm requires the shortest time to run. Therefore, considering the performance-complexity tradeoff, the proposed algorithm is very useful in practical AF MIMO relay systems.

TABLE II
THE COMPUTATION TIME VERSUS N_1, $r_1 = 8$ b/s/Hz, AND $r_2 = 10$ b/s/Hz.

N_1	1	2	3	4	5	6
Proposed	**0.08**	**0.46**	**0.41**	**0.49**	**0.73**	**1.00**
Exhaustive+Algo2	0.08	1.77	4.28	8.94	18.86	42.30
Exhaustive+fmincon	1.35	2.31	6.08	13.28	26.66	55.95

VI. CONCLUSIONS

We have studied the precoding matrices optimization for a two-hop AF MIMO relay system, where the relay node concurrently transmits its own signals and forwards the source signals to the destination node. We have derived the optimal structure of the source and relay matrices for Schur-concave objective functions, which simplifies the original optimization problem to a joint subchannel and power allocation problem. Moreover, QoS constraints have been considered to address the fairness issue. A primal decomposition based algorithm has been developed to efficiently solve the power allocation problem. Simulation results show that compared with the exhaustive search based channel allocation approach and the general nonlinear programming based power allocation algorithm, the proposed subchannel and power allocation algorithms have a much lower computational complexity with only a small performance loss.

APPENDIX A
PROOF OF THEOREM 1

Let us introduce the eigenvalue decomposition (EVD) of

$$\mathbf{A} = \mathbf{H}\mathbf{B}\mathbf{B}^H\mathbf{H}^H = \mathbf{U}_a\mathbf{\Lambda}_a\mathbf{U}_a^H \tag{64}$$

where $\mathbf{\Lambda}_a$ is a diagonal matrix with its diagonal elements sorted in a decreasing order and based on the assumption of Theorem 1, the dimension of $\mathbf{\Lambda}_a$ is $N_1 \times N_1$. Let us also introduce the following two SVDs

$$\mathbf{G}\mathbf{F}_1(\mathbf{H}\mathbf{B}\mathbf{B}^H\mathbf{H}^H + \mathbf{I}_{N_r})^{\frac{1}{2}} = \mathbf{U}_{x_1}\mathbf{\Lambda}_{x_1}\mathbf{V}_{x_1}^H \tag{65}$$

$$\mathbf{G}\mathbf{F}_2 = \mathbf{U}_{x_2}\mathbf{\Lambda}_{x_2}\mathbf{V}_{x_2}^H \tag{66}$$

where $\mathbf{\Lambda}_{x_1}$ and $\mathbf{\Lambda}_{x_2}$ are diagonal matrices with their diagonal elements sorted in a decreasing order and based on the assumption of Theorem 1, the dimensions of $\mathbf{\Lambda}_{x_1}$ and $\mathbf{\Lambda}_{x_2}$ are $N_1 \times N_1$ and $N_2 \times N_2$, respectively. We can obtain from (64)-(66) that

$$[\mathbf{G}\mathbf{F}_1(\mathbf{H}\mathbf{B}\mathbf{B}^H\mathbf{H}^H + \mathbf{I}_{N_r})^{\frac{1}{2}},\ \mathbf{G}\mathbf{F}_2] = \mathbf{U}_x\mathbf{\Lambda}_x\mathbf{V}_x^H \tag{67}$$

$$\mathbf{H}\mathbf{B} = \mathbf{U}_a\mathbf{\Lambda}_a^{\frac{1}{2}}\mathbf{V}_a^H \tag{68}$$

where $\mathbf{V}_a$ is an $N_1 \times N_1$ unitary matrix and

$$\mathbf{U}_x = [\mathbf{U}_{x_1}, \mathbf{U}_{x_2}], \;\; \mathbf{\Lambda}_x = \begin{bmatrix} \mathbf{\Lambda}_{x_1} & \mathbf{0} \\ \mathbf{0} & \mathbf{\Lambda}_{x_2} \end{bmatrix}, \;\; \mathbf{V}_x = \begin{bmatrix} \mathbf{V}_{x_1} & \mathbf{0} \\ \mathbf{0} & \mathbf{V}_{x_2} \end{bmatrix}. \tag{69}$$

From (64), (65), and (68), we obtain that

$$\begin{aligned} \mathbf{GF}_1\mathbf{HB} &= \mathbf{U}_{x_1}\mathbf{\Lambda}_{x_1}\mathbf{V}_{x_1}^H(\mathbf{A}+\mathbf{I}_{N_r})^{-\frac{1}{2}}\mathbf{U}_a\mathbf{\Lambda}_a^{\frac{1}{2}}\mathbf{V}_a^H \\ &= \mathbf{U}_{x_1}\mathbf{\Lambda}_{x_1}\mathbf{P}(\mathbf{\Lambda}_a^{-1}+\mathbf{I}_{N_1})^{-\frac{1}{2}}\mathbf{V}_a^H \end{aligned} \tag{70}$$

where $\mathbf{P} = \mathbf{V}_{x_1}^H\mathbf{U}_a$ is an $N_1 \times N_1$ matrix. Based on (66) and (70), we have

$$[\mathbf{GF}_1\mathbf{HB}, \;\; \mathbf{GF}_2] = \mathbf{U}_x\mathbf{D}\mathbf{V}^H \tag{71}$$

where

$$\mathbf{D} = \begin{bmatrix} \mathbf{\Lambda}_{x_1}\mathbf{P}(\mathbf{\Lambda}_a^{-1}+\mathbf{I}_{N_1})^{-\frac{1}{2}} & \mathbf{0} \\ \mathbf{0} & \mathbf{\Lambda}_{x_2} \end{bmatrix}, \;\; \mathbf{V} = \begin{bmatrix} \mathbf{V}_a & \mathbf{0} \\ \mathbf{0} & \mathbf{V}_{x_2} \end{bmatrix}.$$

Using (67) and (71), the MSE matrix (8) can be written as

$$\begin{aligned} \mathbf{E} &= \mathbf{I}_N - \mathbf{V}\mathbf{D}^H\mathbf{U}_x^H(\mathbf{I}_{N_d}+\mathbf{U}_x\mathbf{\Lambda}_x^2\mathbf{U}_x^H)^{-1}\mathbf{U}_x\mathbf{D}\mathbf{V}^H \\ &= \mathbf{I}_N - \mathbf{V}\mathbf{D}^H((\mathbf{U}_x^H\mathbf{U}_x)^{-1}+\mathbf{\Lambda}_x^2)^{-1}\mathbf{D}\mathbf{V}^H \\ &= \mathbf{I}_N - \mathbf{V}\mathbf{D}^H(\mathbf{\Lambda}_x^{-2}-\mathbf{\Lambda}_x^{-2}(\mathbf{\Lambda}_x^{-2}+\mathbf{U}_x^H\mathbf{U}_x)^{-1}\mathbf{\Lambda}_x^{-2})\mathbf{D}\mathbf{V}^H \\ &= \mathbf{I}_N - \mathbf{V}\mathbf{D}^H\mathbf{\Lambda}_x^{-2}\mathbf{D}\mathbf{V}^H \\ &\quad + \mathbf{V}\mathbf{D}^H\mathbf{\Lambda}_x^{-2}\begin{pmatrix} \mathbf{\Lambda}_{x_1}^{-2}+\mathbf{I}_{N_1} & \mathbf{U}_{x_1}^H\mathbf{U}_{x_2} \\ \mathbf{U}_{x_2}^H\mathbf{U}_{x_1} & \mathbf{\Lambda}_{x_2}^{-2}+\mathbf{I}_{N_2} \end{pmatrix}^{-1}\mathbf{\Lambda}_x^{-2}\mathbf{D}\mathbf{V}^H \end{aligned} \tag{72}$$

where the identity of

$$(\mathbf{A}+\mathbf{BCD})^{-1} = \mathbf{A}^{-1} - \mathbf{A}^{-1}\mathbf{B}(\mathbf{D}\mathbf{A}^{-1}\mathbf{B}+\mathbf{C}^{-1})^{-1}\mathbf{D}\mathbf{A}^{-1}$$

is used to obtain the third equation. It can be seen from (72) that the optimal $\mathbf{U}_{x_1}$ and $\mathbf{U}_{x_2}$ that minimize $f(\mathbf{d}(\mathbf{E}))$ satisfy

$$\mathbf{U}_{x_1}^H\mathbf{U}_{x_2} = \mathbf{0}. \tag{73}$$

Therefore, $\mathbf{U}_x$ in (69) is an $N_d \times N$ semi-unitary matrix with $\mathbf{U}_x^H\mathbf{U}_x = \mathbf{I}_N$. It will be shown later that while the constraint (12) does not depend on $\mathbf{U}_x$, (73) is also optimal for the constraint (13).

Based on (73), (72) can be written as

$$\mathbf{E} = \mathbf{I}_N - \mathbf{V}\begin{bmatrix} \mathbf{D}_1 & \mathbf{0} \\ \mathbf{0} & \mathbf{D}_2 \end{bmatrix}\mathbf{V}^H \tag{74}$$

where

$$\mathbf{D}_1 = (\mathbf{\Lambda}_a^{-1}+\mathbf{I}_{N_r})^{-\frac{1}{2}}\mathbf{P}^H(\mathbf{I}_{N_1}+\mathbf{\Lambda}_{x_1}^{-2})^{-1}\mathbf{P}(\mathbf{\Lambda}_a^{-1}+\mathbf{I}_{N_r})^{-\frac{1}{2}} \tag{75}$$

$$\mathbf{D}_2 = (\mathbf{I}_{N_2}+\mathbf{\Lambda}_{x_2}^{-2})^{-1}. \tag{76}$$

Similar to the Appendix in [10], it can be proven from (74) and (75) that to optimize (11) for a Schur-concave $f(\cdot)$, there are $\mathbf{P} = \mathbf{I}_{N_1}$ (i.e., $\mathbf{V}_{x_1} = \mathbf{U}_a$) and $\mathbf{V} = \mathbf{I}_N$ (i.e., $\mathbf{V}_a = \mathbf{I}_{N_1}$ and $\mathbf{V}_{x_2} = \mathbf{I}_{N_2}$). As will be shown later, such $\mathbf{V}_{x_1}$, $\mathbf{V}_{x_2}$, and $\mathbf{V}_a$ do not affect the constraints (12) and (13).

It can be shown that (68) is valid if and only if $(\mathbf{U}_h^{\perp})^H\mathbf{U}_a = \mathbf{0}$, where $\mathbf{U}_h^{\perp}$ denotes the left singular vectors of $\mathbf{H}$ associated with the zero singular values, and we find that among the possible solutions of $\mathbf{B}$, the optimal $\mathbf{B}$ which minimizes $\mathrm{tr}(\mathbf{B}\mathbf{B}^H)$ is given by

$$\mathbf{B} = \mathbf{V}_h\mathbf{\Lambda}_h^{-1}\mathbf{U}_h^H\mathbf{U}_a\mathbf{\Lambda}_a^{\frac{1}{2}}\mathbf{V}_a^H. \tag{77}$$

From (77), we have

$$\mathrm{tr}(\mathbf{B}\mathbf{B}^H) = \mathrm{tr}(\mathbf{\Lambda}_a^{\frac{1}{2}}\mathbf{U}_a^H\mathbf{U}_h\mathbf{\Lambda}_h^{-2}\mathbf{U}_h^H\mathbf{U}_a\mathbf{\Lambda}_a^{\frac{1}{2}}). \tag{78}$$

Note that (78) does not depend on $\mathbf{U}_x$, $\mathbf{V}_x$, and $\mathbf{V}_a$. Based on [24, 9.H.1.h], the optimal $\mathbf{U}_a$ that minimizes (78) is $\mathbf{U}_a = \mathbf{U}_{h,m}$. Thus, from (77) and $\mathbf{V}_a = \mathbf{I}_{N_1}$, the optimal $\mathbf{B}$ is $\mathbf{B} = \mathbf{V}_{h,m}\mathbf{\Lambda}_{h,m}^{-1}\mathbf{\Lambda}_a^{\frac{1}{2}}$. Therefore, we prove the optimal structure of $\mathbf{B}$ in (14) with $\mathbf{\Lambda}_b = \mathbf{\Lambda}_{h,m}^{-1}\mathbf{\Lambda}_a^{\frac{1}{2}}$.

Similarly, we obtain that (65) and (66) hold if and only if $(\mathbf{U}_g^{\perp})^H\mathbf{U}_x = \mathbf{0}$, where $\mathbf{U}_g^{\perp}$ denotes the left singular vectors of $\mathbf{G}$ associated with the zero singular values, and among the possible solutions of $\mathbf{F}_1$, the optimal $\mathbf{F}_1$ minimizing $\mathrm{tr}(\mathbf{F}_1(\mathbf{H}\mathbf{B}\mathbf{B}^H\mathbf{H}^H+\mathbf{I}_{N_r})\mathbf{F}_1^H)$ is

$$\mathbf{F}_1 = \mathbf{V}_g\mathbf{\Lambda}_g^{-1}\mathbf{U}_g^H\mathbf{U}_{x_1}\mathbf{\Lambda}_{x_1}\mathbf{V}_{x_1}^H\mathbf{U}_a(\mathbf{\Lambda}_a+\mathbf{I}_{N_1})^{-\frac{1}{2}}\mathbf{U}_a^H. \tag{79}$$

From (66), the optimal $\mathbf{F}_2$ minimizing $\mathrm{tr}(\mathbf{F}_2\mathbf{F}_2^H)$ is given by

$$\mathbf{F}_2 = \mathbf{V}_g\mathbf{\Lambda}_g^{-1}\mathbf{U}_g^H\mathbf{U}_{x_2}\mathbf{\Lambda}_{x_2}\mathbf{V}_{x_2}^H. \tag{80}$$

Based on (79) and (80), the power consumption at the relay node is given by

$$\begin{aligned} &\mathrm{tr}(\mathbf{F}_1(\mathbf{H}\mathbf{B}\mathbf{B}^H\mathbf{H}^H+\mathbf{I}_{N_r})\mathbf{F}_1^H+\mathbf{F}_2\mathbf{F}_2^H) \\ &= \mathrm{tr}(\mathbf{\Lambda}_g^{-1}\mathbf{U}_g^H\mathbf{U}_x\mathbf{\Lambda}_x^2\mathbf{U}_x^H\mathbf{U}_g\mathbf{\Lambda}_g^{-1}). \end{aligned} \tag{81}$$

Note that (81) does not depend on $\mathbf{V}_x$ and $\mathbf{V}_a$. Based on [24, 9.H.1.h], the optimal $\mathbf{U}_x$ that minimizes (81) is

$$\mathbf{U}_x = \mathbf{U}_{g,m}\mathbf{\Pi} \tag{82}$$

where $\mathbf{\Pi}$ is an $N \times N$ permutation matrix such that the diagonal elements of $\mathbf{\Pi}\mathbf{\Lambda}_x\mathbf{\Pi}^T$ are sorted in a decreasing order. Therefore, from (69) and (82), we have

$$\mathbf{U}_{x_i} = \mathbf{U}_{g,m}\mathbf{\Pi}_i, \qquad i = 1, 2 \tag{83}$$

where $\mathbf{\Pi}_1$ and $\mathbf{\Pi}_2$ contain the first N_1 and the last N_2 columns of $\mathbf{\Pi}$, respectively. Obviously, $\mathbf{U}_{x_1}$ and $\mathbf{U}_{x_2}$ in (83) satisfy (73).

From (79), (83), and $\mathbf{V}_{x_1} = \mathbf{U}_a = \mathbf{U}_{h,m}$, we have

$$\mathbf{F}_1 = \mathbf{V}_{g,1}\mathbf{\Lambda}_{g,1}^{-1}\mathbf{\Lambda}_{x_1}(\mathbf{\Lambda}_a+\mathbf{I}_{N_1})^{-\frac{1}{2}}\mathbf{U}_{h,m}^H$$

where $\mathbf{V}_{g,1} = \mathbf{V}_{g,m}\mathbf{\Pi}_1$ and $\mathbf{V}_{g,m}$ contains N columns of $\mathbf{V}_g$ associated with the largest N singular values of $\mathbf{G}$. Thus, the optimal structure of $\mathbf{F}_1$ in (14) is proven with $\mathbf{\Lambda}_{f_1} = \mathbf{\Lambda}_{g,1}^{-1}\mathbf{\Lambda}_{x_1}(\mathbf{\Lambda}_a+\mathbf{I}_{N_1})^{-\frac{1}{2}}$. Similarly, from (80), (83), and $\mathbf{V}_{x_2} = \mathbf{I}_{N_2}$, we have

$$\mathbf{F}_2 = \mathbf{V}_{g,2}\mathbf{\Lambda}_{g,2}^{-1}\mathbf{\Lambda}_{x_2}$$

where $\mathbf{V}_{g,2} = \mathbf{V}_{g,m}\mathbf{\Pi}_2$. Therefore, we prove the optimal structure of $\mathbf{F}_2$ in (14) with $\mathbf{\Lambda}_{f_2} = \mathbf{\Lambda}_{g,2}^{-1}\mathbf{\Lambda}_{x_2}$.

APPENDIX B
PROOF OF THEOREM 2

Let us introduce $\xi_i = \frac{a_i x_i}{1+a_i x_i+b_{\mathcal{I}_i} y_i}$, $i = 1, \cdots, N_1$. Obviously, for any $x_i > 0$ and $y_i > 0$, there is $0 < \xi_i < 1$. For *any* $\mathbf{x}$ satisfying (32) and (34), and *any* $\mathcal{I}$ and $\mathcal{J}$ satisfying

(36), the problem (31)-(36) reduces to a problem of optimizing $\mathbf{y}$ and $\mathbf{z}$ given by

$$\max_{\mathbf{y},\mathbf{z}} \sum_{i=1}^{N_1} \log_2(1+\xi_i b_{\mathcal{I}_i} y_i) + \sum_{j=1}^{N_2} \log_2(1+b_{\mathcal{J}_j} z_j) \tag{84}$$

$$\text{s.t.} \sum_{i=1}^{N_1} y_i + \sum_{j=1}^{N_2} z_j \le P_r \tag{85}$$

$$y_i > 0,\ i=1,\cdots,N_1,\ \ z_j > 0,\ j=1,\cdots,N_2. \tag{86}$$

The problem (84)-(86) has the well-known water-filling solution given by

$$y_i = \mu - \frac{1}{\xi_i b_{\mathcal{I}_i}}, \quad i=1,\cdots,N_1 \tag{87}$$

$$z_j = \mu - \frac{1}{b_{\mathcal{J}_j}}, \quad j=1,\cdots,N_2 \tag{88}$$

where μ satisfies the following equation

$$\sum_{i=1}^{N_1}\left(\mu - \frac{1}{\xi_i b_{\mathcal{I}_i}}\right) + \sum_{j=1}^{N_2}\left(\mu - \frac{1}{b_{\mathcal{J}_j}}\right) = P_r. \tag{89}$$

From (87) and (88), the maximum of (84) can be written as

$$M_1 = \sum_{i=1}^{N_1} \log_2(\xi_i b_{\mathcal{I}_i}\mu) + \sum_{j=1}^{N_2} \log_2(b_{\mathcal{J}_j}\mu). \tag{90}$$

By solving (89), we obtain

$$\mu = \frac{1}{N}\left(P_r + \sum_{i=1}^{N_1}\frac{1}{\xi_i b_{\mathcal{I}_i}} + \sum_{j=1}^{N_2}\frac{1}{b_{\mathcal{J}_j}}\right). \tag{91}$$

Now we show that if we swap $b_{\mathcal{I}_i}$ with $b_{\mathcal{J}_j}$ where $b_{\mathcal{I}_i} < b_{\mathcal{J}_j}$ then the maximal value of the objective function (84) will decrease. Without loss of generality, we assume that $b_{\mathcal{I}_1} < b_{\mathcal{J}_1}$ and $b_{\mathcal{I}_1}$ is swapped with $b_{\mathcal{J}_1}$. After the swapping operation, the problem (84)-(86) becomes

$$\max_{\mathbf{y},\mathbf{z}} \sum_{i=2}^{N_2} \log_2(1+\xi_i b_{\mathcal{I}_i} y_i) + \log_2(1+\xi_1 b_{\mathcal{J}_1} y_1) + \sum_{j=2}^{N_2} \log_2(1+b_{\mathcal{J}_j} z_j) + \log_2(1+b_{\mathcal{I}_1} z_1) \tag{92}$$

$$\text{s.t.} \sum_{i=1}^{N_1} y_i + \sum_{j=1}^{N_2} z_j \le P_r \tag{93}$$

$$y_i > 0,\ i=1,\cdots,N_1,\ \ z_j > 0,\ j=1,\cdots,N_2. \tag{94}$$

The solution to the problem (92)-(94) is given by

$$y_1 = \nu - \frac{1}{\xi_1 b_{\mathcal{J}_1}}, \quad z_1 = \nu - \frac{1}{b_{\mathcal{I}_1}} \tag{95}$$

$$y_i = \nu - \frac{1}{\xi_i b_{\mathcal{I}_i}}, \quad i=2,\cdots,N_1 \tag{96}$$

$$z_j = \nu - \frac{1}{b_{\mathcal{J}_j}}, \quad j=2,\cdots,N_2 \tag{97}$$

where ν satisfy the following equation

$$\nu - \frac{1}{\xi_1 b_{\mathcal{J}_1}} + \sum_{i=2}^{N_1}\left(\nu - \frac{1}{\xi_i b_{\mathcal{I}_i}}\right) + \nu - \frac{1}{b_{\mathcal{I}_1}} + \sum_{j=2}^{N_2}\left(\nu - \frac{1}{b_{\mathcal{J}_j}}\right) = P_r. \tag{98}$$

From (98), we obtain

$$\nu = \frac{1}{N}\left(P_r + \frac{1}{\xi_1 b_{\mathcal{J}_1}} + \sum_{i=2}^{N_1}\frac{1}{\xi_i b_{\mathcal{I}_i}} + \frac{1}{b_{\mathcal{I}_1}} + \sum_{j=2}^{N_2}\frac{1}{b_{\mathcal{J}_j}}\right). \tag{99}$$

By substituting (95)-(97) back into (92), the maximum of (92) can be written as

$$M_2 = \sum_{i=2}^{N_1} \log_2(\xi_i b_{\mathcal{I}_i}\nu) + \sum_{j=2}^{N_2} \log_2(b_{\mathcal{J}_j}\nu) + \log_2(\xi_1 b_{\mathcal{J}_1}\nu) + \log_2(b_{\mathcal{I}_1}\nu). \tag{100}$$

Based on (91) and (99), we have

$$\mu - \nu = \frac{1}{N}\left(\frac{1}{\xi_1 b_{\mathcal{I}_1}} + \frac{1}{b_{\mathcal{J}_1}} - \frac{1}{\xi_1 b_{\mathcal{J}_1}} - \frac{1}{b_{\mathcal{I}_1}}\right) = \frac{1}{N}\left(\frac{1}{\xi_1} - 1\right)\left(\frac{1}{b_{\mathcal{I}_1}} - \frac{1}{b_{\mathcal{J}_1}}\right) > 0. \tag{101}$$

From (90), (100), and (101), we can see that

$$M_1 - M_2 = N\log_2\left(\frac{\mu}{\nu}\right) > 0. \tag{102}$$

Through (102), we can conclude that for the problem (31)-(36), the maximum of (31) is achieved when the N_2 largest $b_i, i=1,\cdots,N_2$ are allocated to $\mathbf{s}_r$, i.e., $\mathcal{J}=\{1,\cdots,N_2\}$ and $\mathcal{I}=\{N_2+1,\cdots,N\}$, because any swap between such $b_{\mathcal{I}_i}$ with such $b_{\mathcal{J}_j}$ decreases the maximum of (31).

Appendix C
Proof of Theorem 3

With a given $\mathbf{x}$ satisfying (44), the problem (43)-(45) becomes

$$\max_{\mathbf{y}} \sum_{i=1}^{N_1} \log_2\left(1 + \frac{a_i x_i b_{\mathcal{I}_i} y_i}{1 + a_i x_i + b_{\mathcal{I}_i} y_i}\right) \tag{103}$$

$$\text{s.t.} \sum_{i=1}^{N_1} y_i \le P_y, \quad y_i > 0,\ i=1,\cdots,N_1. \tag{104}$$

Let us define $g(y_i) = \log_2(1 + \frac{a_i x_i b_{\mathcal{I}_i} y_i}{1+a_i x_i + b_{\mathcal{I}_i} y_i})$. The second-order derivative of $g(y_i)$ can be calculated as

$$\nabla^2 g(y_i) = \frac{-a_i x_i b_{\mathcal{I}_i}^2 (2 + a_i x_i + 2 b_{\mathcal{I}_i} y_i)}{\ln 2\ (1 + a_i x_i + b_{\mathcal{I}_i} y_i)^2 (1 + b_{\mathcal{I}_i} y_i)^2}. \tag{105}$$

It can be seen that $\nabla^2 g(y_i) \le 0$. Thus the problem (103)-(104) is a convex problem. According to [30, 5.6.1], $J_1(P_y)$ is a convex function of P_y with any given $\mathbf{x}$ satisfying (44).

Since the problem (46)-(47) is a convex problem. Based on [30, 5.6.1], $J_2(P_y)$ is a convex function of $-P_y$. Since the negative sign of a variable does not change the convexity of a function, we find that $J_2(P_y)$ is a convex function of P_y. Therefore, $J(P_y) = J_1(P_y) + J_2(P_y)$ is a convex function of P_y with any given $\mathbf{x}$ satisfying (44).

ACKNOWLEDGEMENT

The authors would like to thank the editor and anonymous reviewers for their valuable comments and suggestions that helped improve the quality of the paper.

REFERENCES

[1] J. N. Laneman, D. N. C. Tse, and G. W. Wornell, "Cooperative diversity in wireless networks: Efficient protocols and outage behavior," *IEEE Trans. Inf. Theory*, vol. 50, pp. 3062-3080, Dec. 2004.

[2] M. Yuksel and E. Erkip, "Multiple-antenna cooperative wireless systems: A diversity-multiplexing tradeoff perspective," *IEEE Trans. Inf. Theory*, vol. 53, pp. 3371-3393, Oct. 2007.

[3] 3GPP, "Relay architectures for E-UTRA (LTE-Advanced)," Tech. Rep. TR 36.806, Mar. 2010.

[4] L. Sanguinetti, A. A. D'Amico, and Y. Rong, "A tutorial on the optimization of amplify-and-forward MIMO relay systems," *IEEE J. Selet. Areas Commun.*, vol. 30, pp. 1331-1346, Sep. 2012.

[5] B. Wang, J. Zhang, and A. Høst-Madsen, "On the capacity of MIMO relay channels," *IEEE Trans. Inf. Theory*, vol. 51, pp. 29-43, Jan. 2005.

[6] X. Tang and Y. Hua, "Optimal design of non-regenerative MIMO wireless relays," *IEEE Trans. Wireless Commun.*, vol. 6, pp. 1398-1407, Apr. 2007.

[7] O. Muñoz-Medina, J. Vidal, and A. Agustín, "Linear transceiver design in nonregenerative relays with channel state information," *IEEE Trans. Signal Process.*, vol. 55, pp. 2593-2604, June 2007.

[8] W. Guan and H. Luo, "Joint MMSE transceiver design in non-regenerative MIMO relay systems," *IEEE Commun. Lett.*, vol. 12, pp. 517-519, July 2008.

[9] Y. Rong, "Linear non-regenerative multicarrier MIMO relay communications based on MMSE criterion," *IEEE Trans. Commun.*, vol. 58, pp. 1918-1923, July 2008.

[10] Y. Rong, X. Tang, and Y. Hua, "A unified framework for optimizing linear non-regenerative multicarrier MIMO relay communication systems," *IEEE Trans. Signal Process.*, vol. 6, pp. 4837-4851, Dec. 2009.

[11] H. Shen, W. Xu, and C. Zhao, "A semi-closed form solution to MIMO relaying optimization with source-destination link," *IEEE Signal Process. Lett.*, vol. 23, pp. 247-251, Feb. 2016.

[12] Z. He, J. Zhang, W. Liu, and Y. Rong, "New results on transceiver design for two-hop amplify-and-forward MIMO relay systems with direct link," *IEEE Trans. Signal Process.*, vol. 64, pp. 5232-5241, Oct. 2016.

[13] Y. Rong, "Optimal linear non-regenerative multi-hop MIMO relays with MMSE-DFE receiver at the destination," *IEEE Trans. Wireless Commun.*, vol. 9, pp. 2268-2279, Jul. 2010.

[14] M. Ahn, H.-B. Kong, T. Kim, C. Song, and I. Lee, "Precoding techniques for MIMO AF relaying systems with decision feedback receiver," *IEEE Trans. Wireless Commun.*, vol. 14, pp. 446-455, Jan. 2015.

[15] F.-S. Tseng, M.-Y. Chang, and W.-R. Wu, "Robust Tomlinson-Harashima source and linear relay precoders design in amplify-and-forward MIMO relay systems," *IEEE Trans. Commun.*, vol. 60, pp. 1124-1137, Apr. 2012.

[16] Z. He, W. Jiang, and Y. Rong, "Robust design for amplify-and-forward MIMO relay systems with direct link and imperfect channel information," *IEEE Trans. Wireless Commun.*, vol. 14, pp. 353-363, Jan. 2015.

[17] C. Xing, S. Ma, Z. Fei, Y.-C. Wu, and H. V. Poor, "A general robust linear transceiver design for multi-hop amplify-and-forward MIMO relaying systems," *IEEE Trans. Signal Process.*, vol. 61, pp. 1196-1209, Mar. 2013.

[18] L. Sanguinetti, A. A. D'Amico, and Y. Rong, "On the design of amplify-and-forward MIMO-OFDM relay systems with QoS requirements specified as Schur-convex functions of the MSEs," *IEEE Trans. Veh. Technol.*, vol. 62, pp. 1871-1877, May 2013.

[19] Y. Fu, L. Yang, W.-P. Zhu, and C. Liu, "Optimum linear design of two-hop MIMO relay networks with QoS requirements," *IEEE Trans. Signal Process.*, vol. 59, pp. 2257-2269, May 2011.

[20] L. Sanguinetti and A. A. D'Amico, "Power allocation in two-hop amplify-and-forward MIMO relay systems with QoS requirements," *IEEE Trans. Signal Process.*, vol. 60, pp. 2494-2507, May 2012.

[21] S. Berger, M. Kuhn, A. Wittneben, T. Unger, and A. Klein, "Recent advances in amplify-and-forward two-hop relaying," *IEEE Commun. Magazine*, pp. 50-56, Jul. 2009.

[22] C.-B. Chae, T. Tang, R. W. Heath, Jr., and S. Cho, "MIMO relaying with linear processing for multiuser transmission in fixed relay networks," *IEEE Trans. Signal Process.*, vol. 56, pp. 727-738, Feb. 2008.

[23] M. R. A. Khandaker and Y. Rong, "Joint transceiver optimization for multiuser MIMO relay communication systems," *IEEE Trans. Signal Process.*, vol. 60, pp. 5997-5986, Nov. 2012.

[24] A. W. Marshall and I. Olkin, *Inequalities: Theory of Majorization and Its Applications*. Academic Press, 1979.

[25] D. P. Palomar and M. Chiang, "A tutorial on decomposition methods for network utility maximization," *IEEE J. Sel. Areas. Commun.*, vol. 24, pp. 1439-1451, Aug. 2006.

[26] T. Kong and Y. Hua, "Optimal design of source and relay pilots for MIMO relay channel estimation," *IEEE Trans. Signal Process.*, vol. 59, pp. 4438-4446, Sep. 2011.

[27] Y. Rong, M. R. A. Khandaker, and Y. Xiang, "Channel estimation of dual-hop MIMO relay systems via parallel factor analysis," *IEEE Trans. Wireless Commun.*, vol. 11, pp. 2224-2233, June 2012.

[28] A. Antoniou and W.-S. Lu, *Practical Optimization: Algorithms and Engineering Applications*. Spring Street, NY: Springer Science+Business Media, LCC, 2007.

[29] D. P. Palomar, J. M. Cioffi, and M. A. Lagunas, "Joint Tx-Rx beamforming design for multicarrier MIMO channels: A unified framework for convex optimization," *IEEE Trans. Signal Process.*, vol. 51, pp. 2381-2401, Sep. 2003.

[30] S. Boyd and L. Vandenberghe, *Convex Optimization*. Cambridge, U.K.: Cambridge Univ. Press, 2004.

PLACE PHOTO HERE

Qiao Su (S'16) received the M.S. degree from the College of Communications Engineering, PLA University of Science and Technology in 2015, where he is currently pursuing the Ph.D. degree with the College of Communications Engineering, Army Engineering University of PLA. His research interests include wireless communications and blind signal processing.

PLACE PHOTO HERE

Yue Rong (S'03-M'06-SM'11) received the Ph.D. degree (summa cum laude) in electrical engineering from the Darmstadt University of Technology, Darmstadt, Germany, in 2005.

He was a Post-Doctoral Researcher with the Department of Electrical Engineering, University of California, Riverside, from February 2006 to November 2007. Since December 2007, he has been with the Department of Electrical and Computer Engineering, Curtin University, Bentley, Australia, where he is currently a Professor. His research interests include signal processing for communications, wireless communications, underwater acoustic communications, applications of linear algebra and optimization methods, and statistical and array signal processing. He has published over 160 journal and conference papers in these areas.

Dr. Rong was a recipient of the Best Paper Award at the 2011 International Conference on Wireless Communications and Signal Processing, the Best Paper Award at the 2010 Asia-Pacific Conference on Communications, and the Young Researcher of the Year Award of the Faculty of Science and Engineering at Curtin University in 2010. He is an Associate Editor of the IEEE TRANSACTIONS ON SIGNAL PROCESSING. He was an Editor of the IEEE WIRELESS COMMUNICATIONS LETTERS from 2012 to 2014, a Guest Editor of the IEEE JOURNAL ON SELECTED AREAS IN COMMUNICATIONS special issue on theories and methods for advanced wireless relays, and was a TPC Member for the IEEE ICC, IEEE GlobalSIP, WCSP, IWCMC, EUSIPCO, and ChinaCom.